N 341 72—07

PAPERS PRESENTED BY JAPAN
AT THE MEETING ON VOID COEFFICIENT
OF HEAVY WATE RMODERATED BOILING
LIGHT WATER COOLED REACTORS, PARIS.
18—20 SEPT. 1972

NUCLEAR DESIGN OF PROTOTYPE HEAVY WATER REACTOR (FUGEN)

September, 1972

Power Reactor and Nuclear Fuel
Development Corporation, Tokyo, Japan

Nuclear Design of Prototype Heavy Water Reactor (FUGEN)

September, 1972

Yoshio WATARI*
Hidemasa KATO**

For an initial core of FUGEN plant, reactivity coefficients are estimated as follows: fuel temperature coefficient is estimated at $(-1.6 \pm 0.4) \times 10^{-5}$ $\Delta k/k/^{\circ}C$; void coefficient, $(-2.0 \pm 3.0) \times 10^{-5}$ $\Delta k/k/\%$ void fraction respectively. The power coefficient is expected to be negative in both initial and equilibrium core.

The reactivity is controlled with 49 control rods, while the excess reactivity which is necessary to burn up is suppressed with the liquid poison in the moderator. Worth of total control rods for initial core is calculated at 14% $\Delta k/k$ with design margin of 2% $\Delta k/k$.

Refueling will be started after one and a half years from the initial reactor operation. The average refueling time and the average discharge exposure are approximately 25 days/4 assemblies and 17,000 MWD/TU for 1.5 E.UO_2 fuel.

Xenon stability and hydrodynamic stability are examined. And it is found that xenon instability will not occur and also hydrodynamic flow instability will not occur.

---

* Hitachi Works, Hitachi Ltd., Hitachi-shi, Ibaraki-ken

** Power Reactor and Nuclear Fuel Development Corporation, Tokyo

Part I. Nuclear Static Analysis

Contents

1. Outline of The Advanced Thermal Reactor FUGEN

FUGEN is the prototype advanced thermal reactor designed to generate 165 MWe. It is a pressure tube type reactor which is moderated by heavy water and cooled by boiling light water. It is under construction in Fukui Prefecture in Japan and its first criticality is expected in June 1975.

Figure 1 shows the vertical section of the reactor. The calandria is a vertical and cylindrical tank which contains 224 pressure tubes, the heavy water moderator and the radial and the axial reflectors. It also incorporates an annular space into which part of the moderator can be dumped to provide reactor shutdown. There are two independent recirculation loops, each of which has 112 pressure tubes, in order to make the reactivity change small in case of loss of coolant accident.

Fuel assemblies are changed from the bottom of the core by a refueling machine without shutting down the reactor.

On-power refueling is the most important long-term method of controlling reactivity when the reactor has reached a condition of equilibrium.

There are 49 control rods in the core and these are inserted from the top of the core through control rod guide tubes. Figure 2 shows the control rod structure. The control rod assembly consists of 81 B_4C rods and is suspended by a cable wound around a drum.

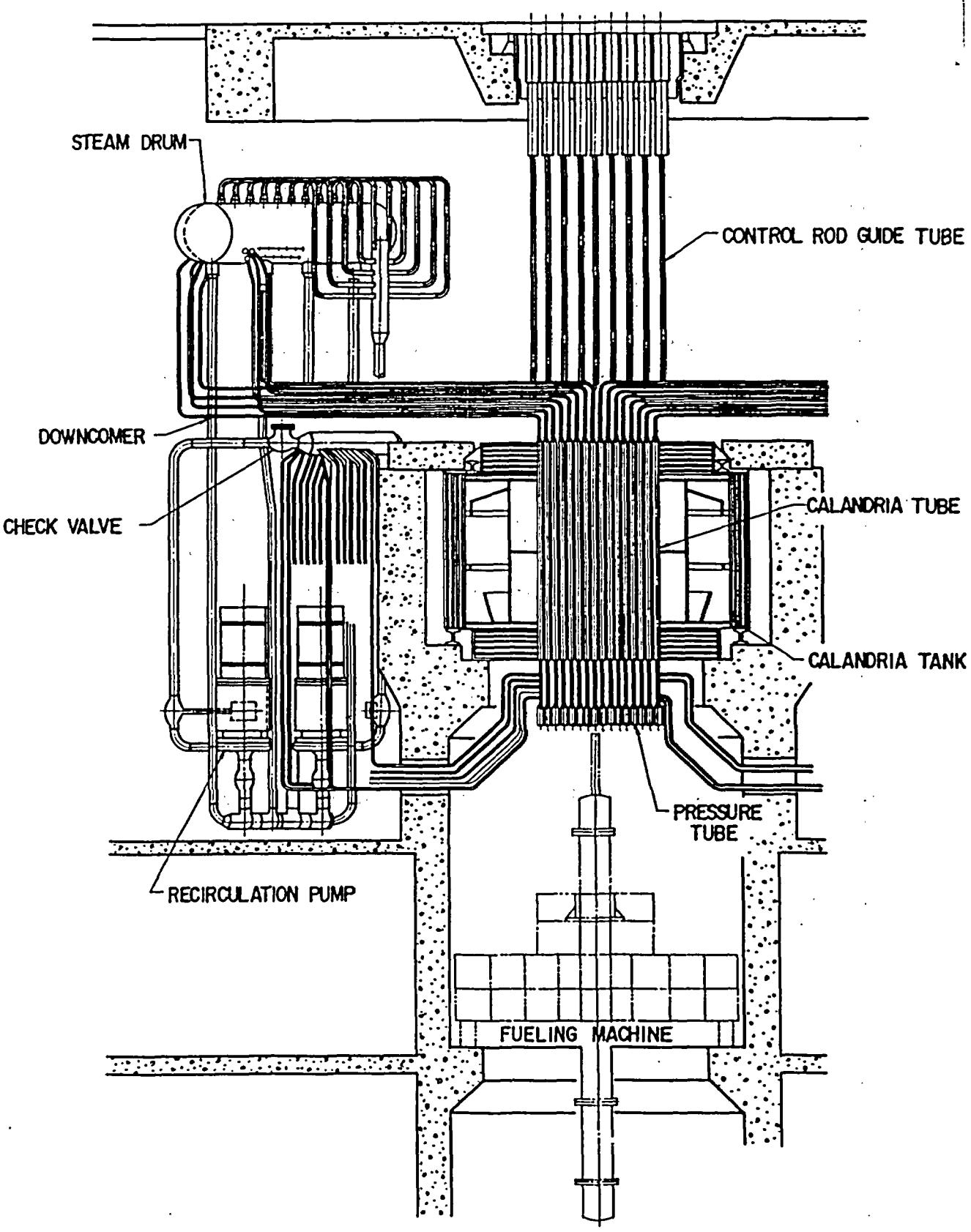

Fig. 1 VERTICAL SECTION REACTOR FUGEN

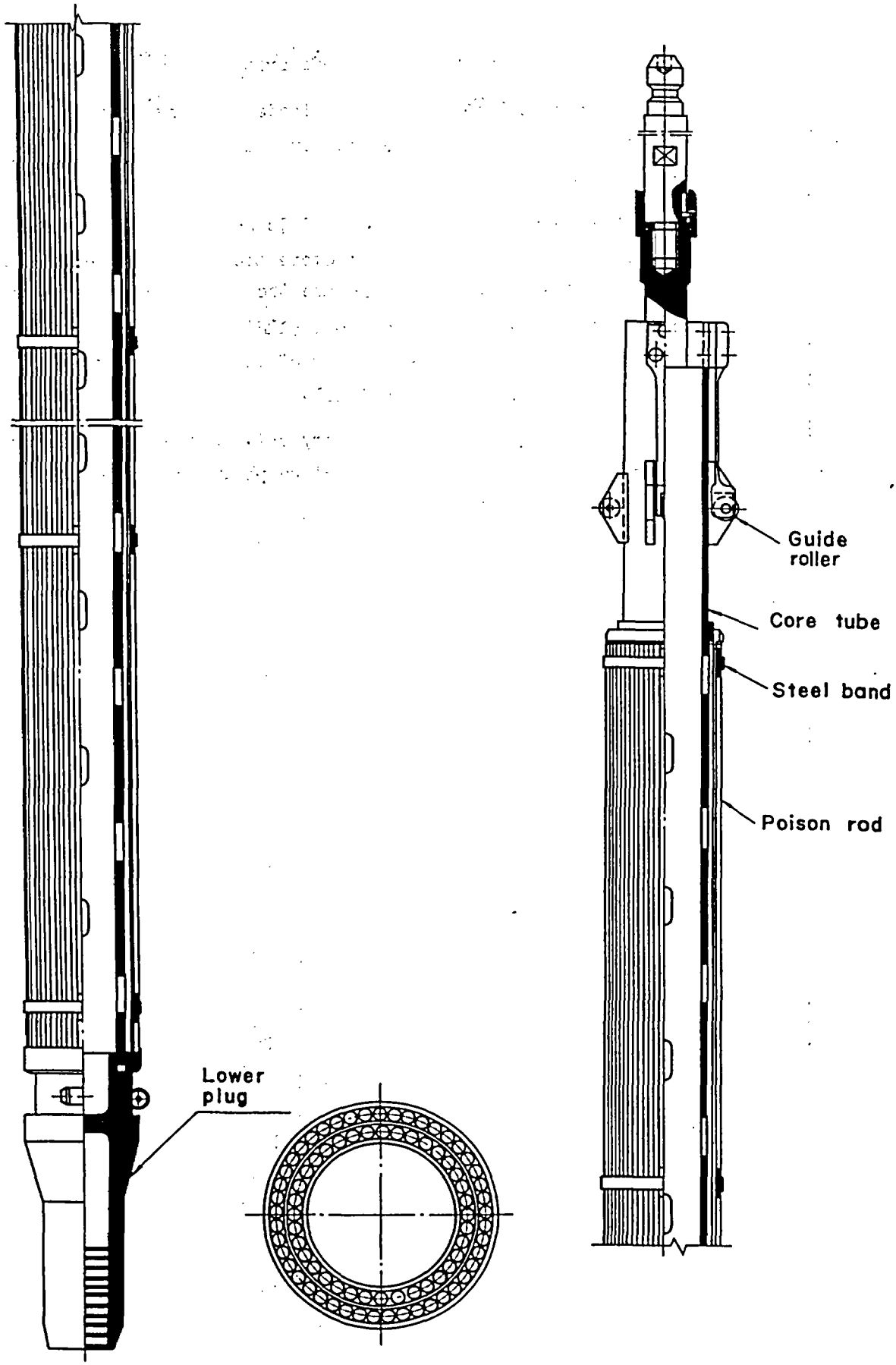

Fig. 2 Control rod structure

Figure 3 shows the core configuration.

The core consists of 2 fuel loaded regions. The inner region is a slightly plutonium-mixed natural uranium and the outer a 1.5 % enriched uranium fuel.

There are 49 control rods and 74 neutron detectors in the core. There are three kinds of neutron detectors according to the reactor power level. The 4 and 6 detectors of these are the source range monitors (SRM) and the intermediate power range monitors (IRM), respectively. The dotted marks in Figure 3 represent the strings of the local power range monitors (LPRM) and each has 4 monitors vertically.

A neutron source is necessary only in the initial start-up operation of the reactor and the self-supplied photo-neutron source is used for start-up after this.

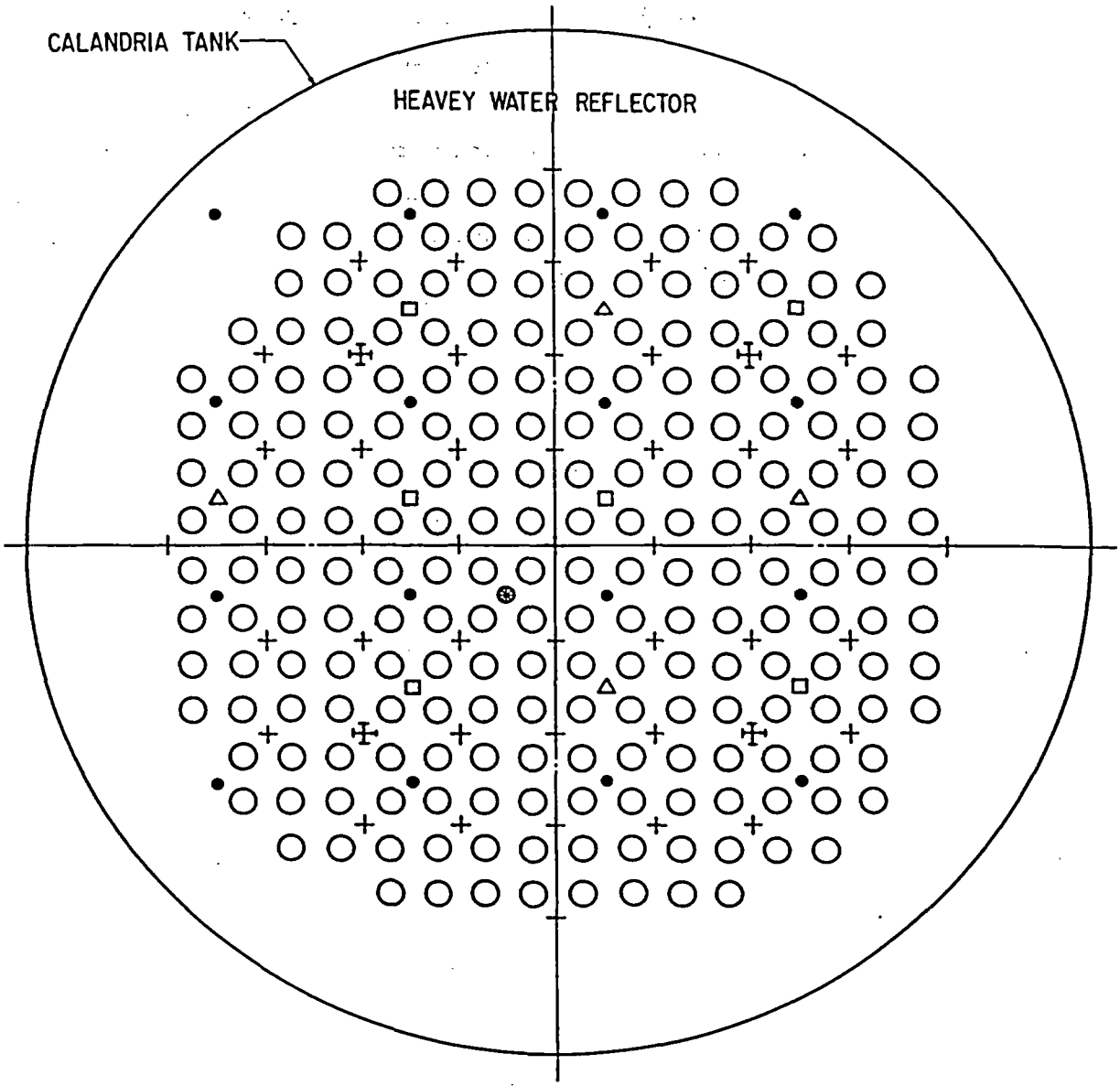

○	FUEL ASSEMBLY	224	•	LPRM	16 x 4
+	CONTROL ROD	45	□	IRM	6
⊹	REGULATING ROD	4	△	SRM	4
⊛	NEUTRON SOURCE	1			

Fig. 3 CORE CONFIGURATION

Figure 4 shows the cross section of the fuel assembly. The fuel rods are arranged in three concentric layers and the number in each layer is 4, 8 and 16 from the center of the cluster. The remaining space in the pressure tube is filled with boiling light water coolant. The core average void fraction in coolant is about 35 percent. The outside of the pressure tube is composed of the thermal insulation, calandria tube and moderator.

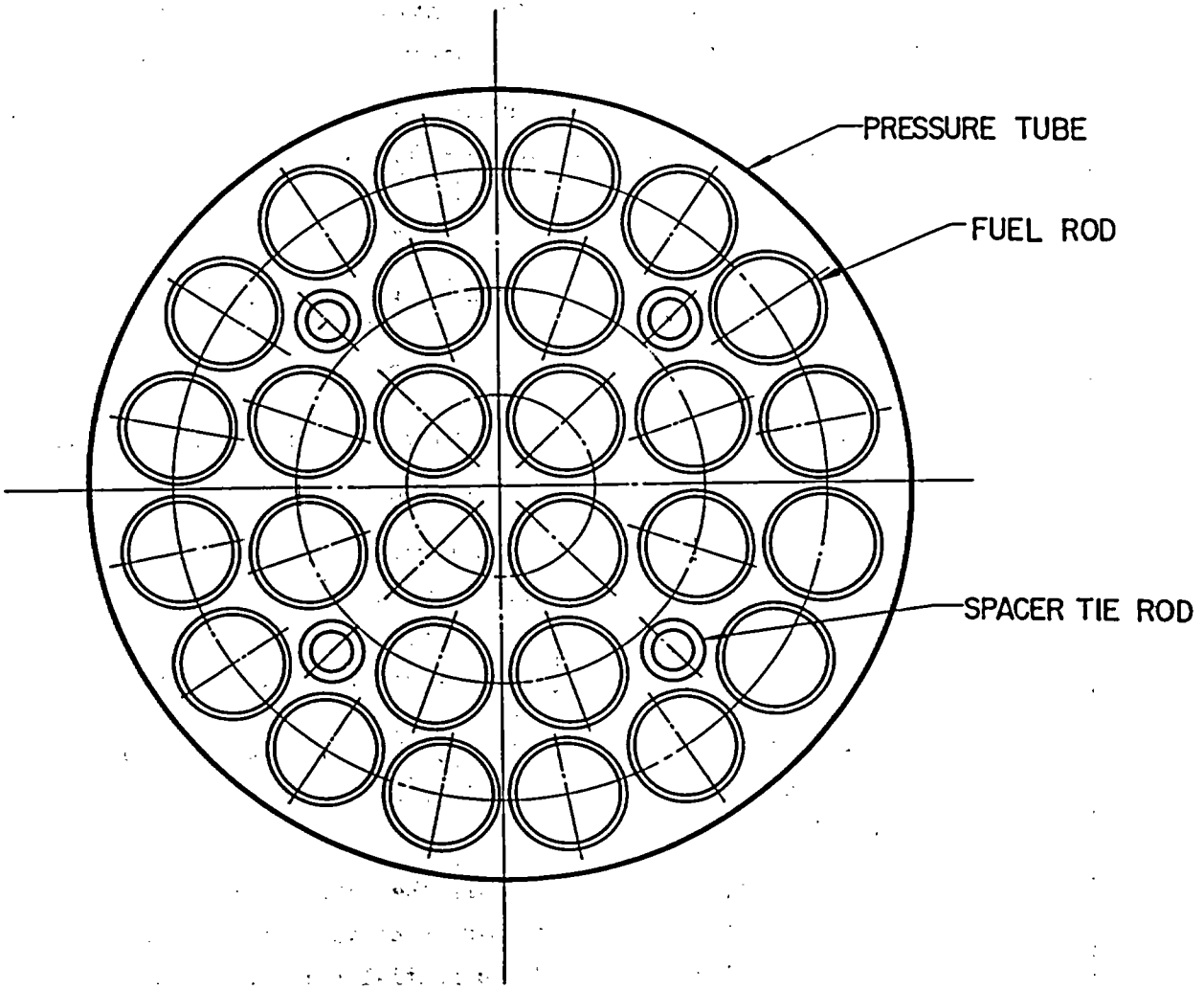

Fig. 4 FUEL ELEMENT

2. Reactivity Coefficients

Table 1 shows coolant void, fuel temperature and moderator temperature coefficient of FUGEN initial core. The error estimated in each reactivity coefficient is derived from comparison with the DCA experiments and the calculated results of the various codes.

In Table 1, moderator temperature coefficient of initial core are positive because of the liquid poison B^{10} in the heavy water moderator.

The power coefficient is composed of the above three reactivity coefficients and is calculated as follows:

$$\text{Power Coefficient} = \sum_i W_i (a_i \pm \Delta a_i)$$

$$= \sum_i W_i a_i \pm \left\{ \sum_i (W_i \Delta a_i)^2 \right\}^{\frac{1}{2}}$$

$$= -(4.5 \pm 1.6) \times 10^{-5} (\Delta k/k)/\% \text{ power}$$

, where a_i : reactivity coefficient in Table 1,

Δa_i : the error of a_i

W_i : weighting factor and
0.2 for void coefficient,
3.8 for temperature coefficient,
0.18 for moderator temperature coefficient.

From the above consideration, the power coefficient for the initial core is negative even if estimated with various errors of each reactivity coefficient.

In the equilibrium core, all the fuel assemblies have plutonium elements. Thus the coolant void reactivity in the equilibrium core is small compared with that of the initial core; also the moderator temperature is negative.

So, the power coefficient and the full core void reactivity in the equilibrium core are more negative than those of the initial core.

Table 1. Reactivity Coefficients

Reactivity Coefficients	Initial Core	Unit
Coolant Void	$(-2.0 \pm 3.0) \times 10^{-5}$	$(\Delta k/k)$ /% void
Fuel Temperature	$(-1.6 \pm 0.4) \times 10^{-5}$	$(\Delta k/k)$ /°C
Moderator Temperature	$(1.1 \pm 0.1) \times 10^{-4}$	$(\Delta k/k)$ /°C

3. Method of Reactivity Control

Because of using slightly enriched fuel the initial core of FUGEN has much excess reactivity. It is impossible to suppress these excess reactivities by the control rods alone. Thus a liquid poison, B^{10}, is used in the initial core to supplement the insufficiency of the control reactivity.

The reactor is shut down by the dump of the heavy water moderator when the control rods can not be inserted in the core.

The control capacity of the control rods, liquid poison and the dump of moderator is as follows:

3.1 Control Rod Worth

There are 49 control rods in the core. Their structure and their positions in the core are shown in Fig. 3 and Fig. 4. The control rod worth at the position indicated in Fig. 6 and the shim rod worth are shown in Tables 4 and 5.

Because of the control rod interaction, the shim rod worth at the time when the flattening rods are inserted is larger than at the time when the flattening rods are not inserted. The total control rods worth in initial and equilibrium core is 14% ($\Delta k/k$) and 15 % ($\Delta k/k$), respectively.

Table 4. Control Rod Worth in Initial and Equilibrium Core

%(Δ k/k)

rod position	Initial Core	Equilibrium Core
1	0.58	0.56
3	0.31	0.52
5	0.03	0.25

Table 5. Shim Rods Worth in Initial and Equilibrium Core

% (Δk/k)

	In the case of 4 shim rods insertion only	In the case of 4 shim rods and flattening rods insertion
Initial Core	0.76	1.15
Equilibrium Core	0.97	1.10

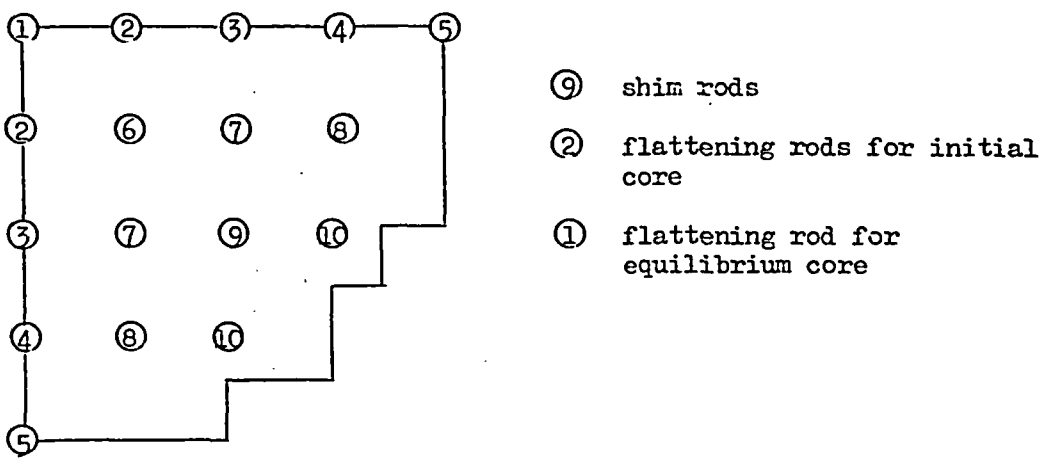

Fig. 6. Control Rod Position

3.2 Liquid Poison Worth

The liquid poison, B^{10}, is added in the moderator to suppress the excess reactivity in the initial core. Its concentration in the moderator is about 7 ppm, is decreased with fuel burn up and is held at 0 ppm after the first refueling.

The liquid poison worth is nearly proportional to its concentration in the moderator as shown in Fig. 7.

3.3 Emergency Scram by The Dump of Moderator

In such a case when by some accident the control rods can not be inserted in the core, the reactor is shut down by the dump of moderator.

In a large reactor, a rapid negative reactivity is added to the core as the moderator level decreases.

The relation between k_{eff} and the dump level of the moderator is shown in Fig. 8.

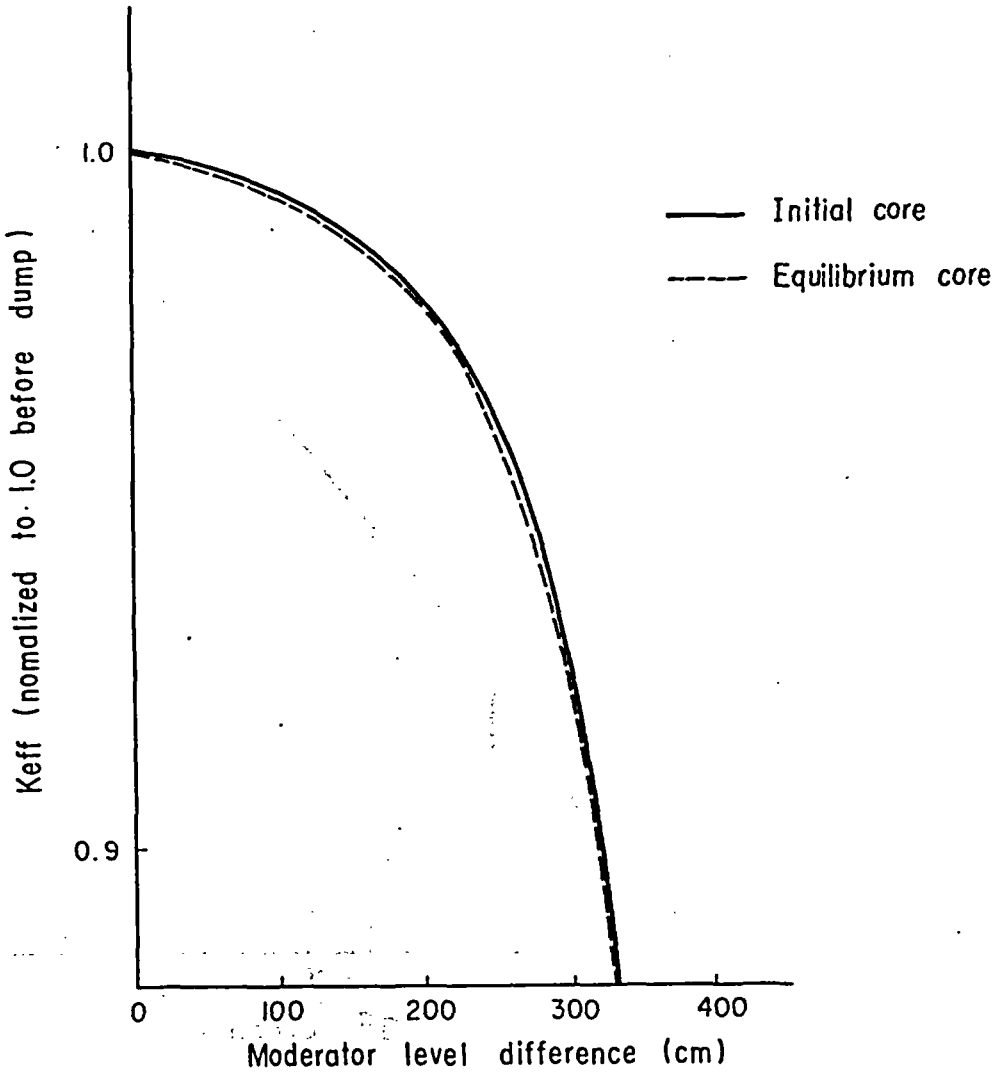

Fig. 8 Keff vs moderator level

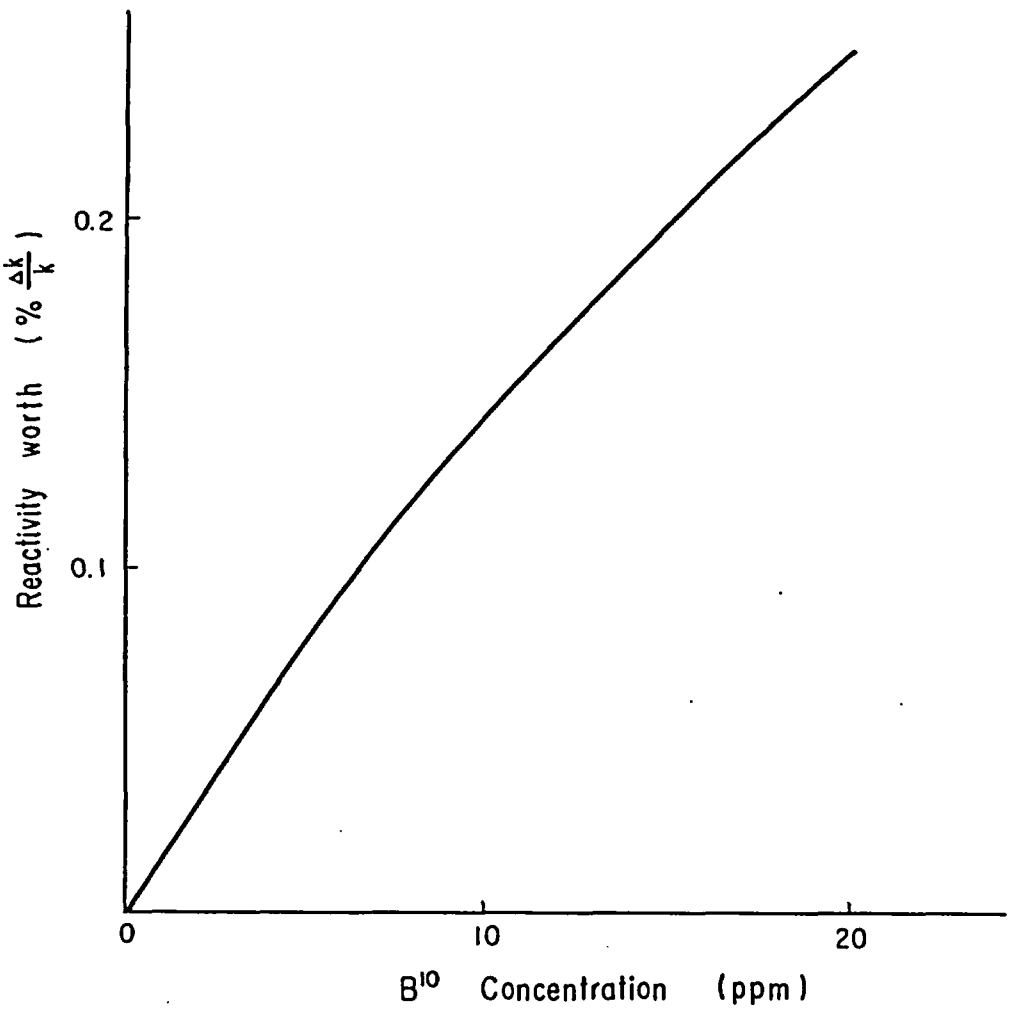

Fig. 7 Liquid Poison Worth vs B^{10} concentration

3.4 Requirements of The Control Rod Worth

The requirements of the control rod worth for initial and equilibrium core are shown in Table 6.

As the calculated worth of the control rods for initial and equilibrium core is 14 %(Δ k/k)and 15 %(Δ k/k), there is about 20 % design margin for control rods because of the combined uncertainties in both the control requirements and the worth of the control rods.

Table 6. Requirements of The Control Rod Worth

	reactivity % (Δ k/k)
Cold to Full Power	2
Build Up of Xe and Sm	4
Fuel Burnup	1
Operating Margin	2
Shutdown Margin	3
T o t a l	12

4. Fuel Management

On-power refueling commences after one and a half years from the initial reactor operation. It is the most important long-term method of controlling reactivity in the equilibrium core.

The limitations of refueling are as follows:

(1) the gross peaking factor ≤ 2.13

(2) minimum critical heat flux ratio > 1.9

(3) maximum linear heat rate ≤ 17.5 kw/ft

(4) the resident time of fuel in core ≤ 5 years

(5) maximum discharge exposure of fuel assembly $\leq 30,000$ MWD/TU

(6) maximum discharge exposure of pellet $\leq 40,000$ MWD/TU

Furthermore, it is desirable to change four fuel assemblies in 90° rotational symmetry at the same time, from the point of LPRM positions in the core.

A representative refueling schedule to satisfy the above limitations is shown in Fig. 9.

The number of fuel assemblies replaced in each refueling is assumed to be four. The average refueling time and the average discharge exposure are about 25 days and 17,000 MWD/TU for the refueling of 1.5% EUO_2. They are stretched more if the radial shuffling of fuel is possible for refueling.

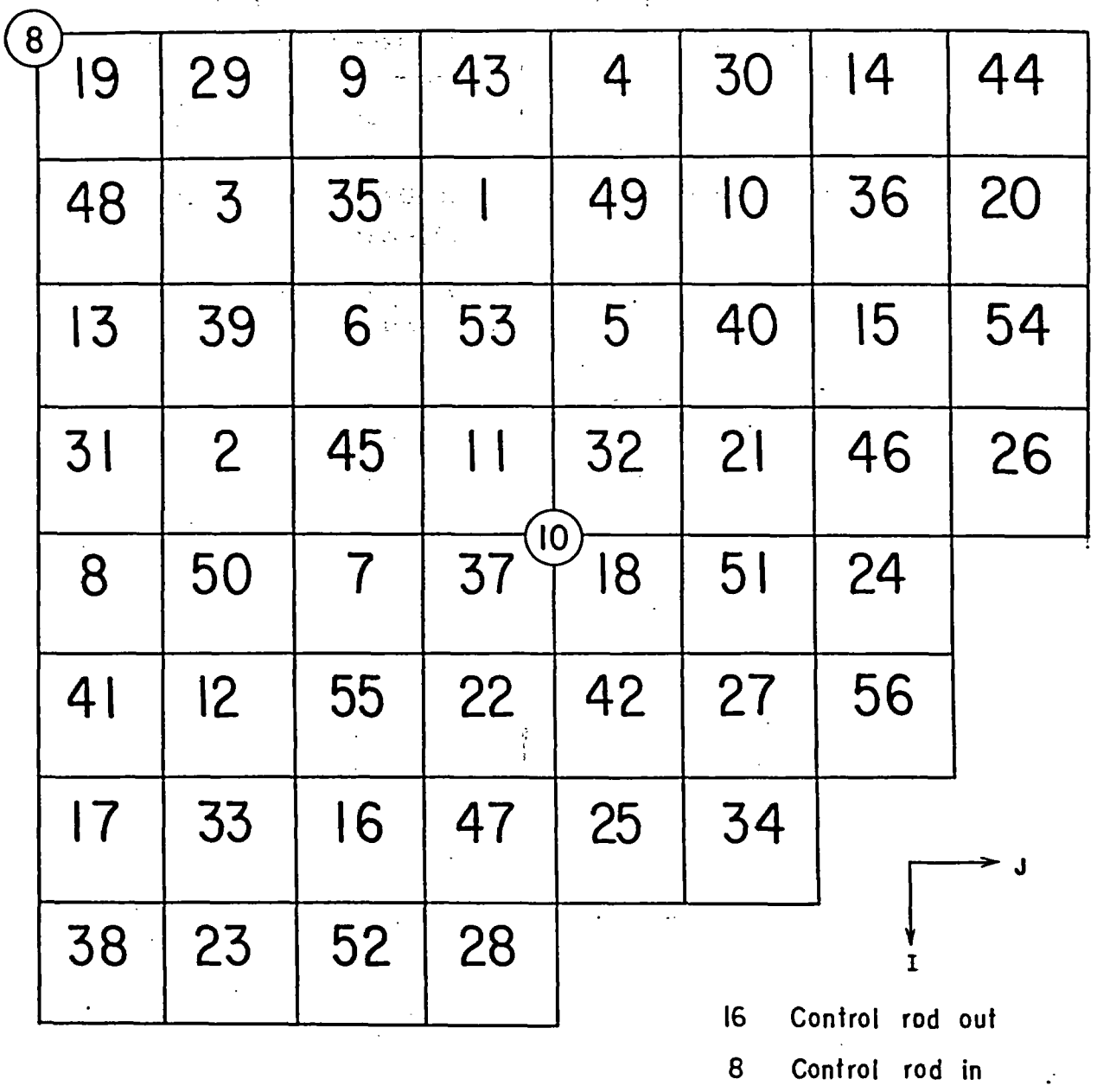

Fig. 9 Representative Refueling Schedule

5. Reactor Stability

Xenon stability and hydrodynamic stability are examined. Xenon oscillation is analyzed by the three-dimensional nuclear thermal hydraulic analysis code, "LAYMON". It is found in the analysis that xenon instability will not occur under the conditions of the reactor size, neutron flux level and power coefficient specified in the design. Also, hydrodynamic flow instability does not occur under the designed condition of pressure loss in the inlet and outlet tube and steam quality.

In Part II of this series, xenon stability by the perturbation of the control rods in equilibrium core is analyzed.

Part II. Nuclear Dynamic Analysis

C o n t e n t s

1. Xenon Oscillation Studies

C o n t e n t s

List of Figures

Number	Title
11	Change of Eigenvalue at Various Times in Equilibrium Core induced by the Half-Insertion (time = 0 hr) and Withdrawal (time = 6 hr) of Power-Flattening Rod and Power-Controlling Rods
12	Radial Xenon Distribution at Various Times during the Three-Dimensional Transient induced by the Half-Insertion (time = 0 hr) and Withdrawal (time = 6 hr) of Power-Flattening Rod and Power-Controlling Rods
13	Radial Xenon Distribution at Various Times during the Three-Dimensional Transient induced by the Half-Insertion (time = 0 hr) and Withdrawal (time = 6 hr) of Power-Flattening Rod and Power-Controlling Rods
14	Axial Xenon Distribution at Various Times during the Three-Dimensional Transient induced by the Half-Insertion (time = 0 hr) and Withdrawal (time = 6 hr) of Power-Flattening Rod and Power-Controlling Rods
15	Axial Xenon Distribution at Various Times during the Three-Dimensional Transient induced by the Half-Insertion (time = 0 hr) and Withdrawal (time = 6 hr) of Power-Flattening Rod and Power-Controlling Rods
16	Axial Xenon Distribution at Various Times during the Three-Dimensional Transient induced by the Half-Insertion (time = 0 hr) and Withdrawal (time = 6 hr) of Power-Flattening Rod and Power-Controlling Rods
17	Axial Xenon Distribution at Various Times during the Three-Dimensional Transient induced by the Half-Insertion (time = 0 hr) and Withdrawal (time = 6 hr) of Power-Flattening Rod and Power-Controlling Rods
18	Axial Xenon Distribution at Various Times during the Three-Dimensional Transient induced by the Half-Insertion (time = 0 hr) and Withdrawal (time = 6 hr) of Power-Flattening Rod and Power-Controlling Rods

1.1 Introduction

The delayed production of Xe^{135} through the decay of I^{135}, which is produced by the fission of a fissile isotope, constitutes a delayed local "reactivity" mechanism which can induce instability in the spatial power distribution if the reactor core dimension is sufficiently large compared with a neutron mean-free-path. This phenomenon has been recognized and widely discussed in technical literature for many years. We have studied the instability with xenon oscillation using the "Improved" LAYMON Code; three-dimensional nuclear thermal hydraulic analysis code improved to be able to calculate also the problem of xenon instability.

In this paper, the three-dimensional analyses of the xenon transients in the 'FUGEN' equilibrium core induced by the control rod motions are carried out using the code.

Xenon instabilities are investigated in three cases; first, half-insertion of the power-flattening rod, second, half-insertion of the power-flattening rod and withdrawal of this rod six hours later, and lastly, half-insertion of both power-flattening rod and power-controlling rods and withdrawal of these rods six hours later. However the reactor has the characteristics of 90-degree rotational symmetry.

It is shown from these cases that the xenon oscillations induced by the control rod motions will not occur in the equilibrium core.

It is necessary in future however to investigate the xenon instabilities induced by the non-symmetric refueling or non-symmetric control-rods operation.

1.2 Description of the "Improved" LAYMON Code

The LAYMON Code is the FLARE type code, which has been improved in order to solve the various nuclear-design problems of the Advanced Thermal Reactor.

The flow chart of the LAYMON Code is shown in Fig. 1.

This LAYMON Code is improved to be able to calculate the xenon-instability problem. Our principal improvements are described below.

From the flow chart of the Subroutine 'FLAREB' in the "Improved" LAYMON Code, and the following equations, we can understand immediately that our principal improvements are made in the Subroutine 'FLAREB', performing

nuclear calculation, and that the degree of reactivity change induced by the transient of xenon concentration is proportional to the xenon concentration at that time.

In this Code, the infinite multiplication factor of the core under consideration, is described below. (See eq. (1), (2), (3))

$$k_\infty = (\text{Rod-controlled } k_\infty) \times Z \quad \text{----- (1)}$$

$$Z = \left\{ 1 - \left(\frac{\Delta k}{k}\right)_{Doppler} - \left(\frac{\Delta k}{k}\right)_{Xenon} \right\} \times \left\{ 1 - \left(\frac{\Delta k}{k}\right)_{Exposure} \right\} \quad \text{----- (2)}$$

where k_∞ is the infinite multiplication factor, proportional to Z, and $\left(\frac{\Delta k}{k}\right)_{Doppler}$, $\left(\frac{\Delta k}{k}\right)_{Xenon}$, $\left(\frac{\Delta k}{k}\right)_{Exposure}$ is the reactivity loss with Doppler effect, Xenon concentration, Exposure, respectively. And also (Rod-controlled k_∞) is k_∞ for which the operation of control rod is taken into account. And $(\Delta k/k)_{Xenon}(t)$ has linear-dependency of xenon concentration at that time, t, i.e.

$$\left(\frac{\Delta k}{k}\right)_{Xenon}(t) = \left(\frac{\Delta k}{k}\right)_{XEN(\infty)} \cdot \frac{XEN(t)}{XEN(\infty)} \quad \text{------ (3)}$$

where XEN(t), XEN (∞) is the xenon concentration at time, t, and in the equilibrium state, respectively, and $\left(\frac{\Delta k}{k}\right)_{XEN(\infty)}$ is the reactivity loss in the equilibrium state.

The flow chart of subroutine 'FLAREB' is shown in Fig. 2.

Fig. 1 Flow Chart of the 'Improved' LAYMON Code

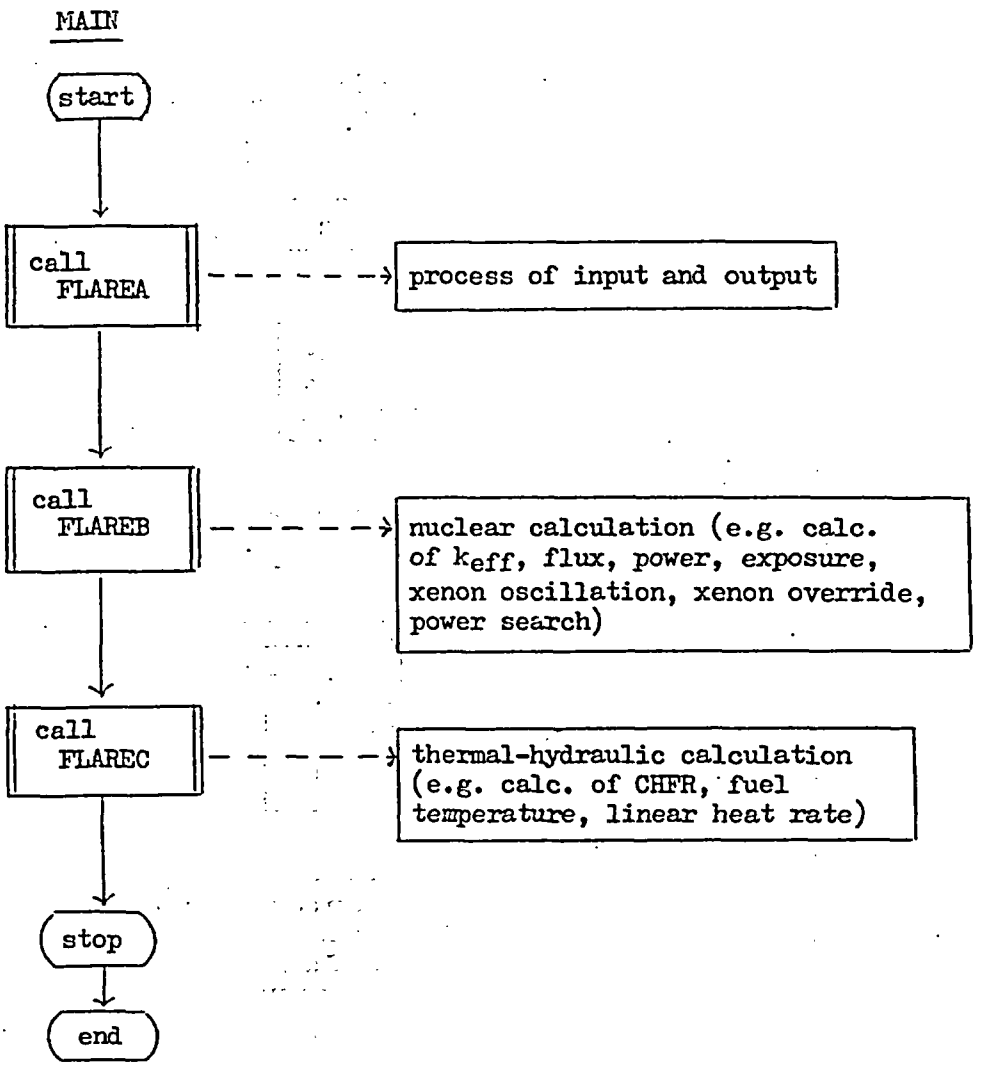

Fig. 2 Flow Chart of Subroutine 'FLAREB'

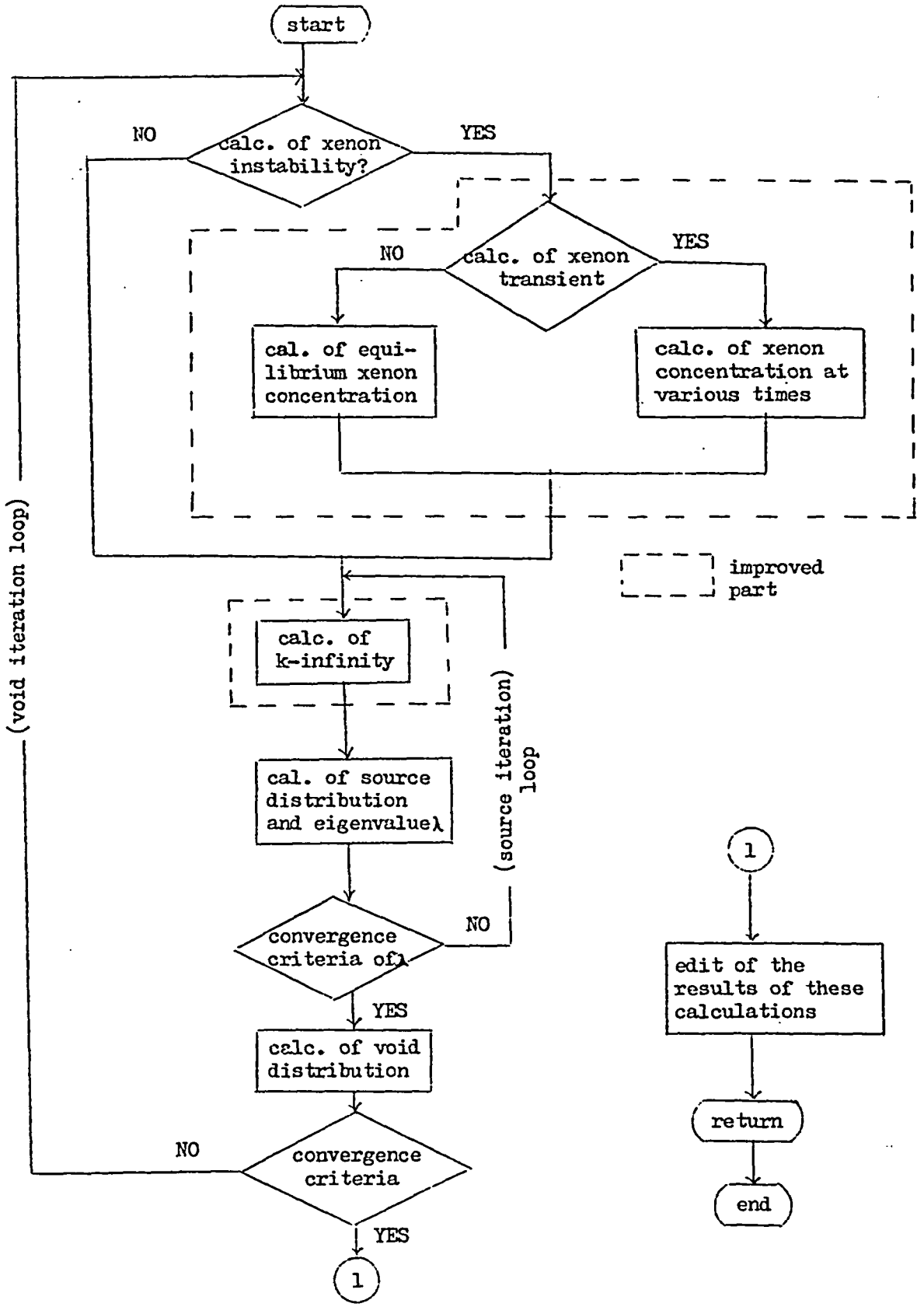

1.3 Three-Dimensional Analysis

LAYMON calculates a nodal power density for a three-dimensional xyz core geometry. The model is based on a modification to one-group diffusion theory in which only the parameters k_∞ and migration area M^2 are involved. An additional simplification involves the replacement of the reflector by an albedo at the core surface so that only mesh points within the active fueled region are considered.

In this paper, the insertion and withdrawal of the power-flattening or power-controlling rods are considered as a disturbance in the reactor. This disturbance has the effect of a decrease (increase) of the xenon concentration in the neighbourhood according to the increase (decrease) of the neutron flux, and may result in the xenon-induced spatial power oscillations.

So, using the "Improved" LAYMON Code, whether such oscillations cease in the end or not, has been examined with the analysis of the xenon and flux transient in the 'FUGEN' equilibrium core, assumed that the exposure of 0.5 % enriched plutonium fuels in the whole core is uniform at 5000 MWD/TU.

Results of the various xenon transients are analyzed in each case.

In this paper, FUGEN has 90-degree rotational symmetry in all cases, and this results in the computer-time-reduction, but this also provides restraint, in not being able to insert or withdraw of control rod in any channel. And it is necessary that the problem of the xenon transients is solved in the whole core system.

The geometry used in the analysis is as follows.

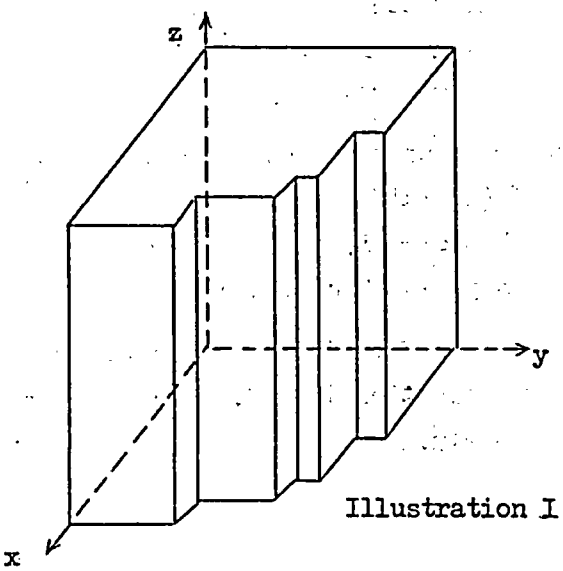

Illustration I

From the illustrations I, II below, any node is decided by the number set (i, j, k), where i, j and k are integral numbers in x, y and z direction respectively. In this paper, i, j has any integral number within the limits of 8, and k, similarly, within the limits of 16.

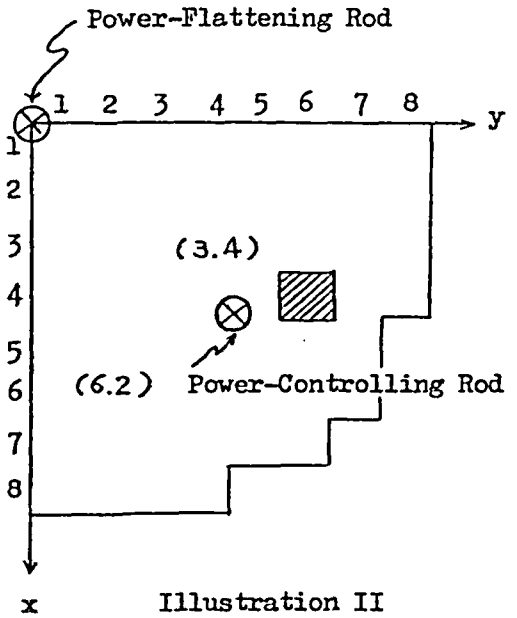

Illustration II

Next, the word 'channel' is decided by the number set (i, j); that is, this is a set of all nodes in z direction. For example, (4, 6) channel is the 'shaded' square region. Illustration II is the geometry solved in this paper.

Case 1. Half-Insertion of the Power-Flattening Rod

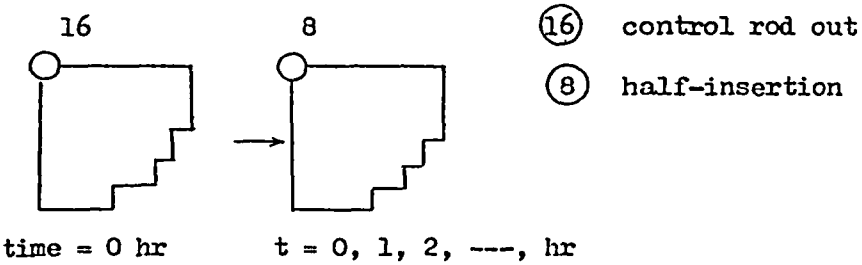

Fig. 3 and Fig. 4 show the neutron flux transient in axial and radial direction, respectively. It is recognized that the fluctuation of the neutron flux due to the insertion of Power-Flattening Rod decreases and is settled down several hours after the rod-insertion.

And also the transient of xenon concentration is shown in Fig. 5 (axial direction) and Fig. 6 (radial direction). It is shown that xenon-concentration transient in this case is settled down completely in the initial xenon-distribution shape at about 20 hours after the rod-insertion.

The power and k-infinity distribution have a similar tendency. In this case, k-infinity is proportional to Z, which is proportional to xenon concentration approximately.

Case 2. Half-Insertion (time = 0 hr) and Withdrawal (time = 6 hr) of the Power-Flattening Rod

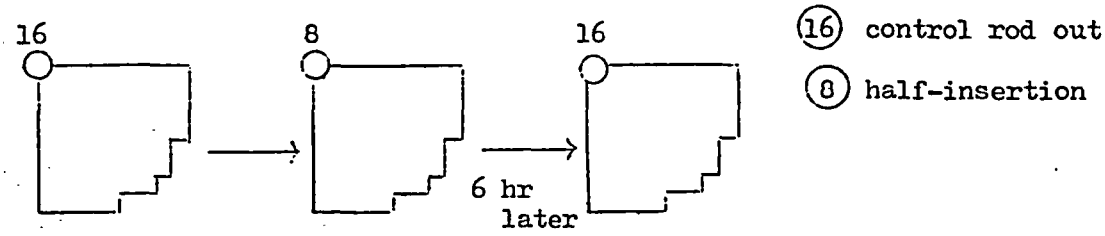

It is shown in Fig. 7 and Fig. 8 that the flux distributions in both axial and radial directions return to the initial distributions due to the withdrawal of the Power-Flattening Rod at once, but slight power oscillation due to the fluctuation of xenon lasts several hours.

The peak of xenon concentration decreases rapidly according to the rod-withdrawal and moves into the lower-half core, to settle down in a few decades.

The difference between Case 1 and Case 2 is the existence of very slight xenon oscillation and movement of the xenon-concentration peak.

Case 3. Half-Insertion (time = 0 hr) and Withdrawal (time = 6 hr) of the Power-Flattening and Controlling Rods

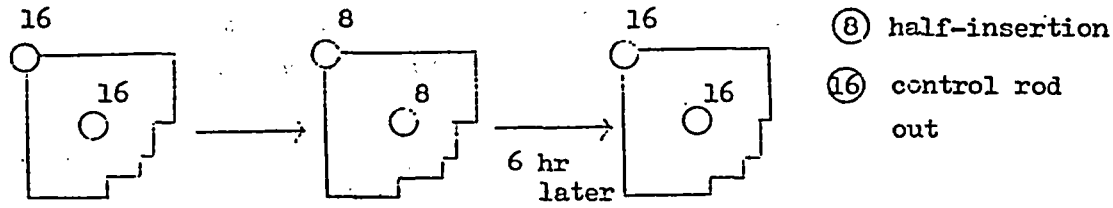

The operations of control rods are shown above. Fig. 11 shows the change of eigenvalue at various times induced by the perturbation of the control-rod operations. From this figure it is immediately recognized that the influence of the control-rod operation vanishes about 20 hours after the control-rod insertion.

It is demonstrated in Fig. 12 and Fig. 13 that the radial xenon-concentration transient settles down in a few decades and radial xenon oscillation does not occur.

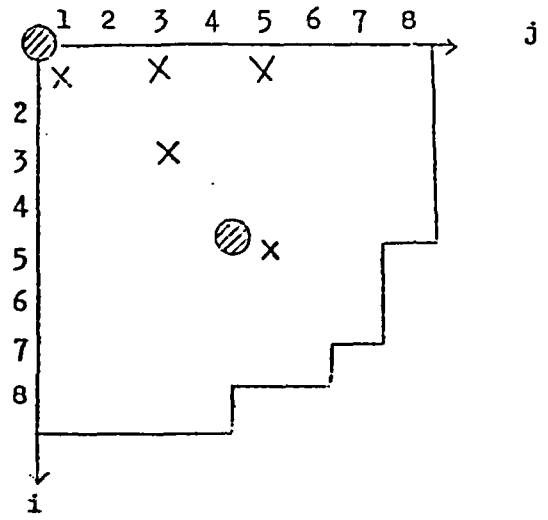

Illustration III

Fig. 14 to Fig. 16 indicate xenon transients in (1, 1), (1, 3), (1, 5) channel respectively. Similarly Fig. 17 and Fig. 18 indicate xenon transients in (3, 3), (5, 5) channel respectively. (See Illustration III). In Fig. 14 to Fig. 16 it is shown that xenon-concentration transients induced the control-rod operations to spread their environments, but their disturbances are smaller as their distances from the rod-operating position are farther away. This tendency can be seen in Fig. 17 to Fig. 18. And, according to the problem of the radial xenon-concentrations transients described above, these xenon transients also settle down from the point of xenon transient propagation.

It is shown in Fig. 15 to Fig. 18 that the azimuthal xenon oscillation cannot occur in this case and the axial xenon-concentration transient also settles down completely in a few decades.

Therefore, it is believed certain that the xenon oscillation induced by the disturbances (e.g. refueling and control rod operation) will not occur in the 'FUGEN' reactor.

Fig. 3 Axial Flux Distribution at Various Times during the Three-Dimensional Transient induced by the Insertion of Power-Flattening Rod in the (1, 1) Channel

(i, j) = (1, 1)

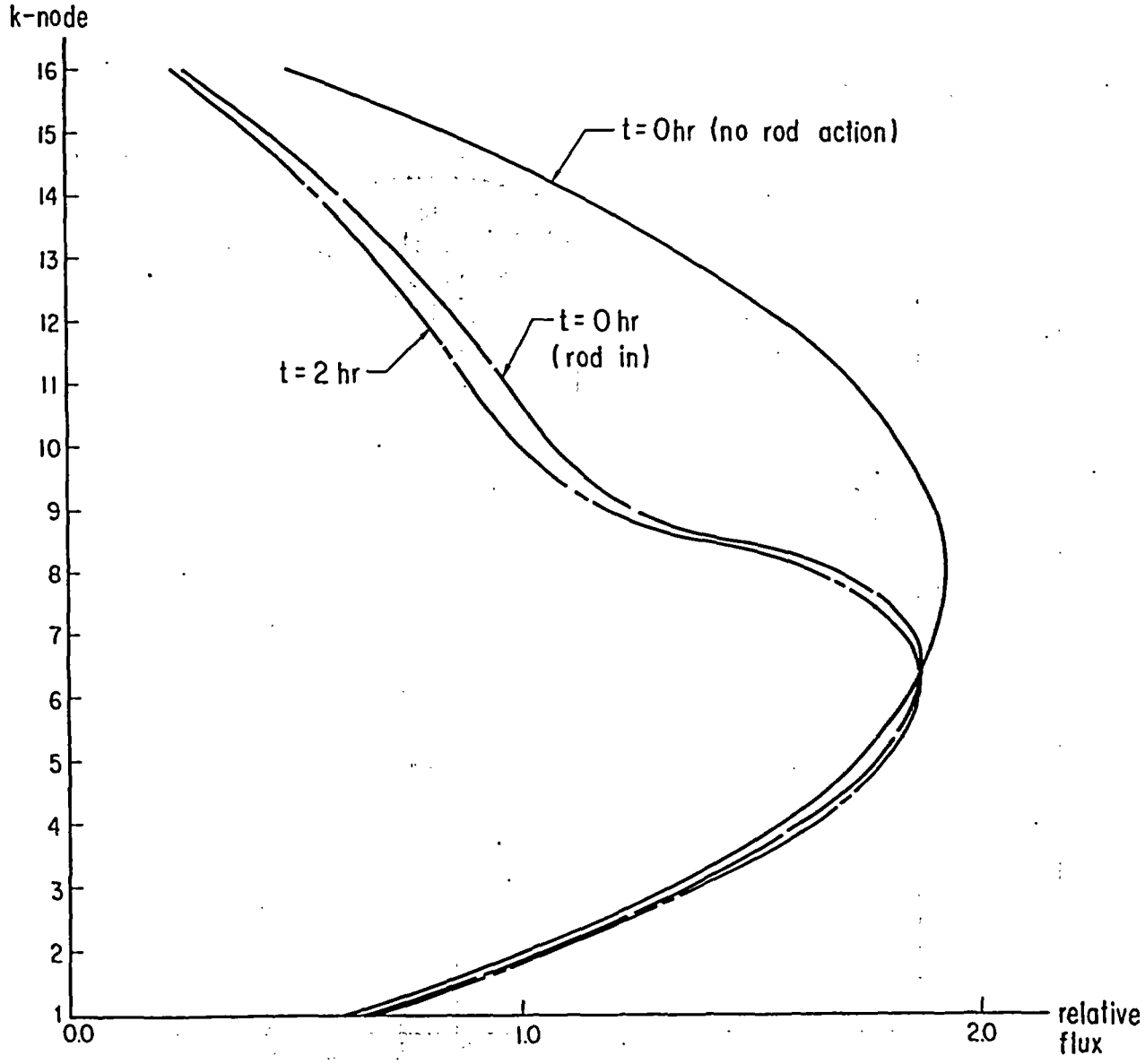

Fig. 4 Radial Flux Distribution at Various Times during the Three-Dimensinal Transient induced by the Insertion of Power-Flattening Rod in the (1, 1) Channel

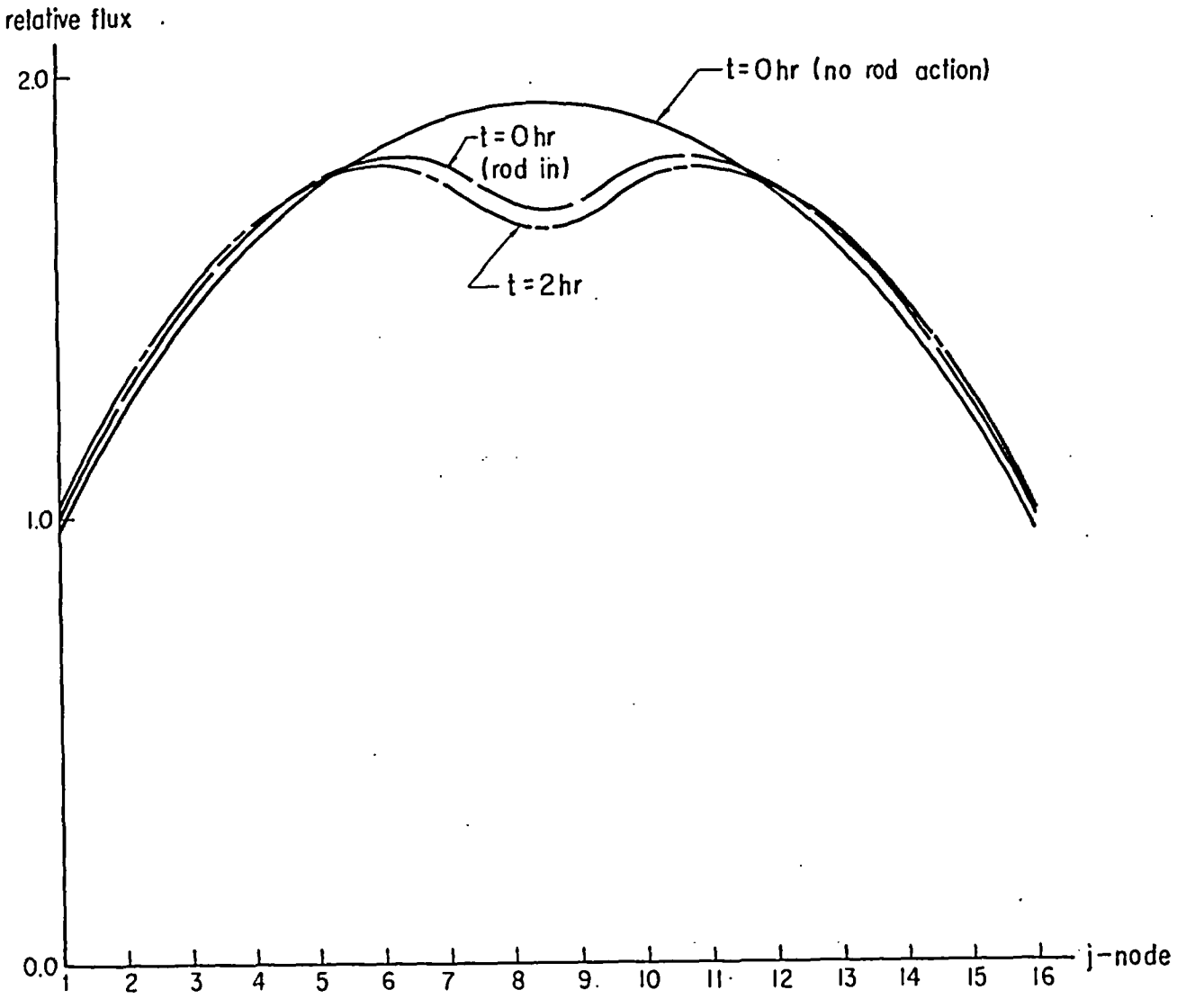

Fig. 5 Axial Xenon Distribution at Various Times during the Three-Dimensional Transient induced by the Insertion of Power-Flattening Rod in the (1, 1) Channel

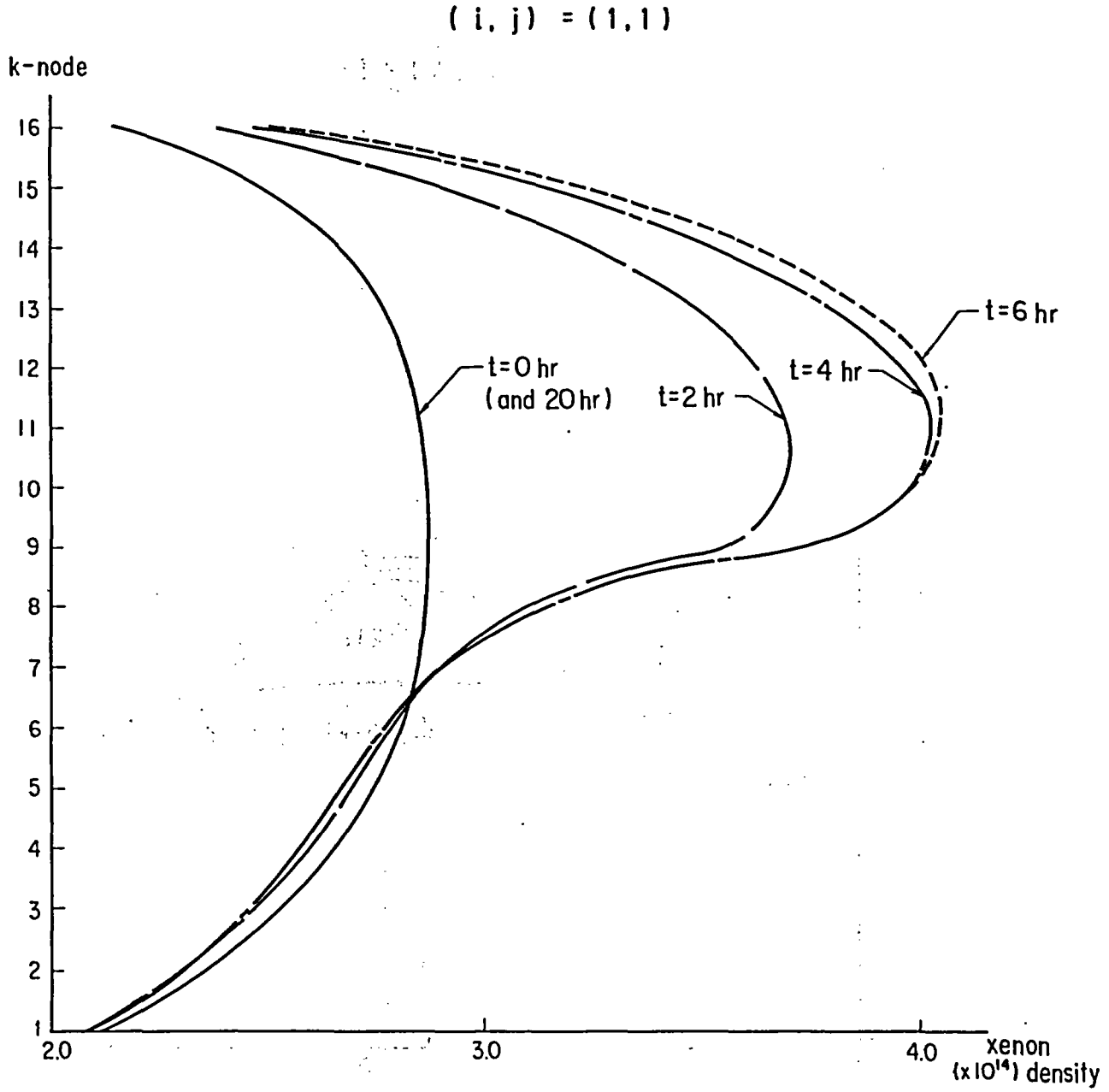

Fig.6 Radial Xenon Distribution at Various Times during the Three - Dimensinal Transient induced by the Insertion of Power Flattening Rod in the (1 , 1) Channel

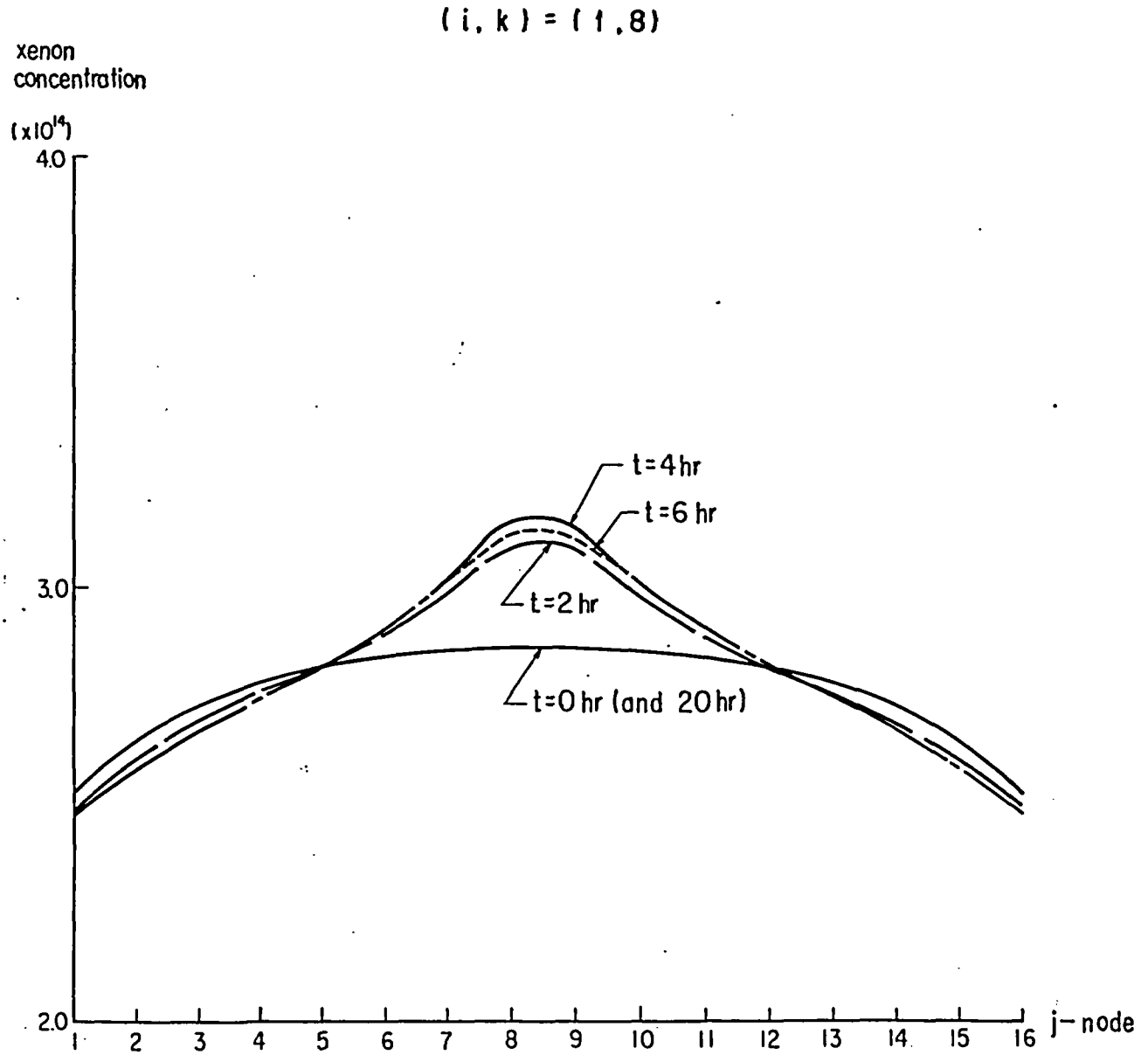

Fig.7 Axial Flux Distribution at Various Times during the Three-Dimensional Transient induced by the Half-Insertion (time = 0 hr) and Withdrawal (time = 6 hr) of the Flattening Rod in the (1, 1) Channel

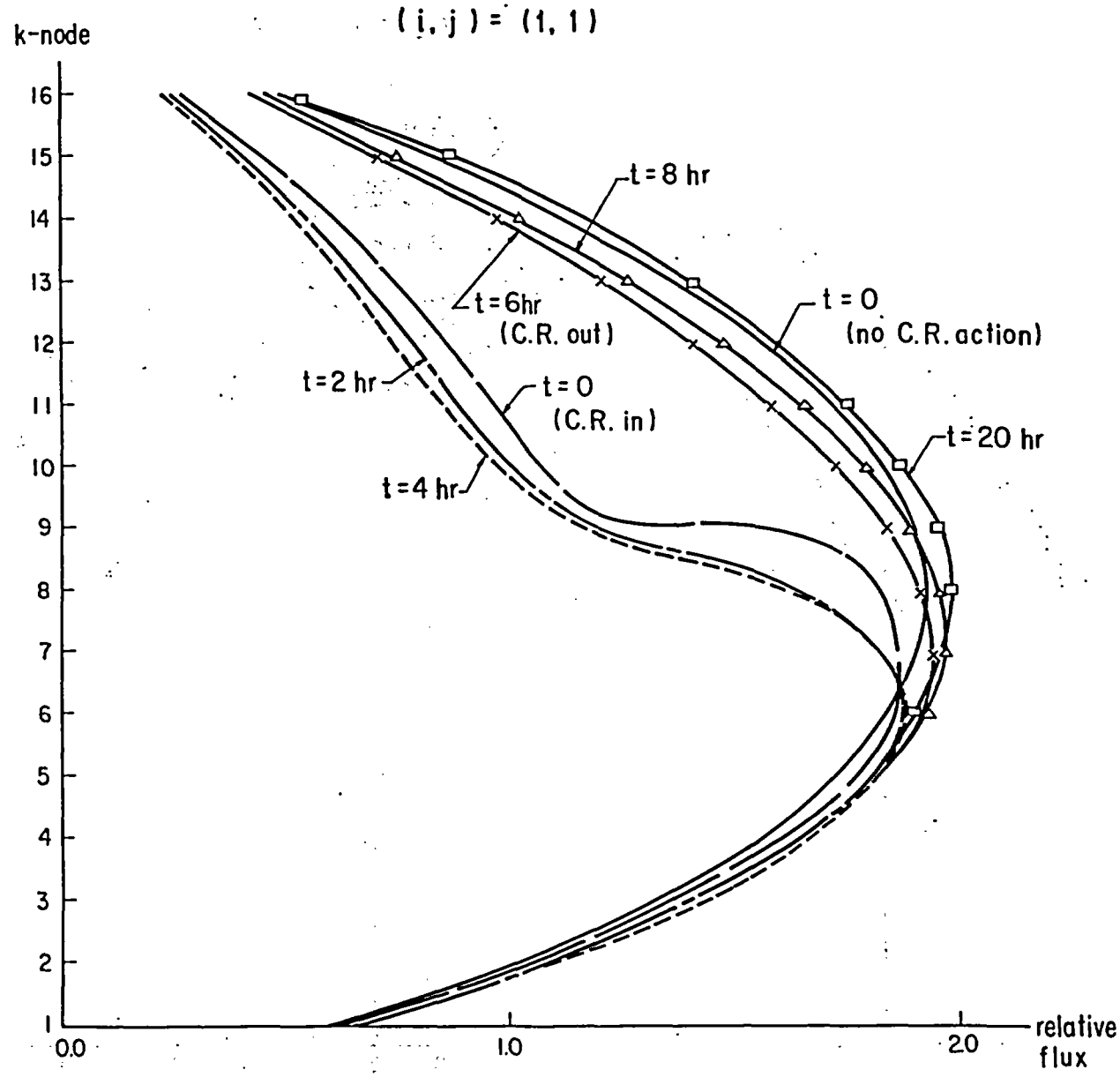

Fig.8 Radial Flux Distribution at Various Times during the Three-Dimensional Transient induced by the Half-Insertion (time = 0 hr) and Withdrawal (time = 6 hr) of the Power-Flattening Rod in the (1, 1) Channel

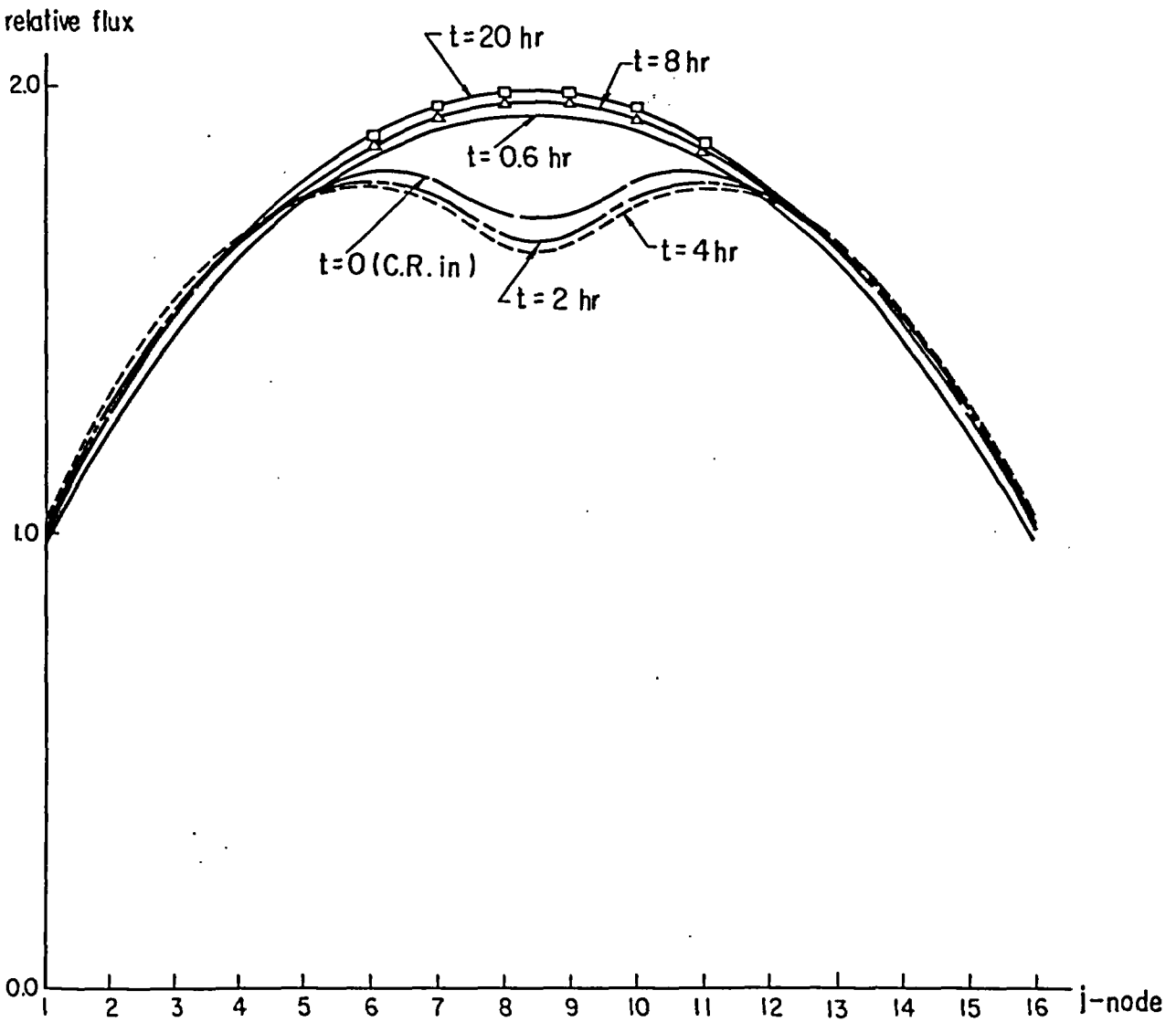

Fig. 9 Axial Xenon Distribution at Various Times during the Three-Dimensional Transient induced by the Half-Insertion (time = 0 hr) and Withdrawal (time = 6 hr) of the Power-Flattening Rod in the (1, 1) Channel

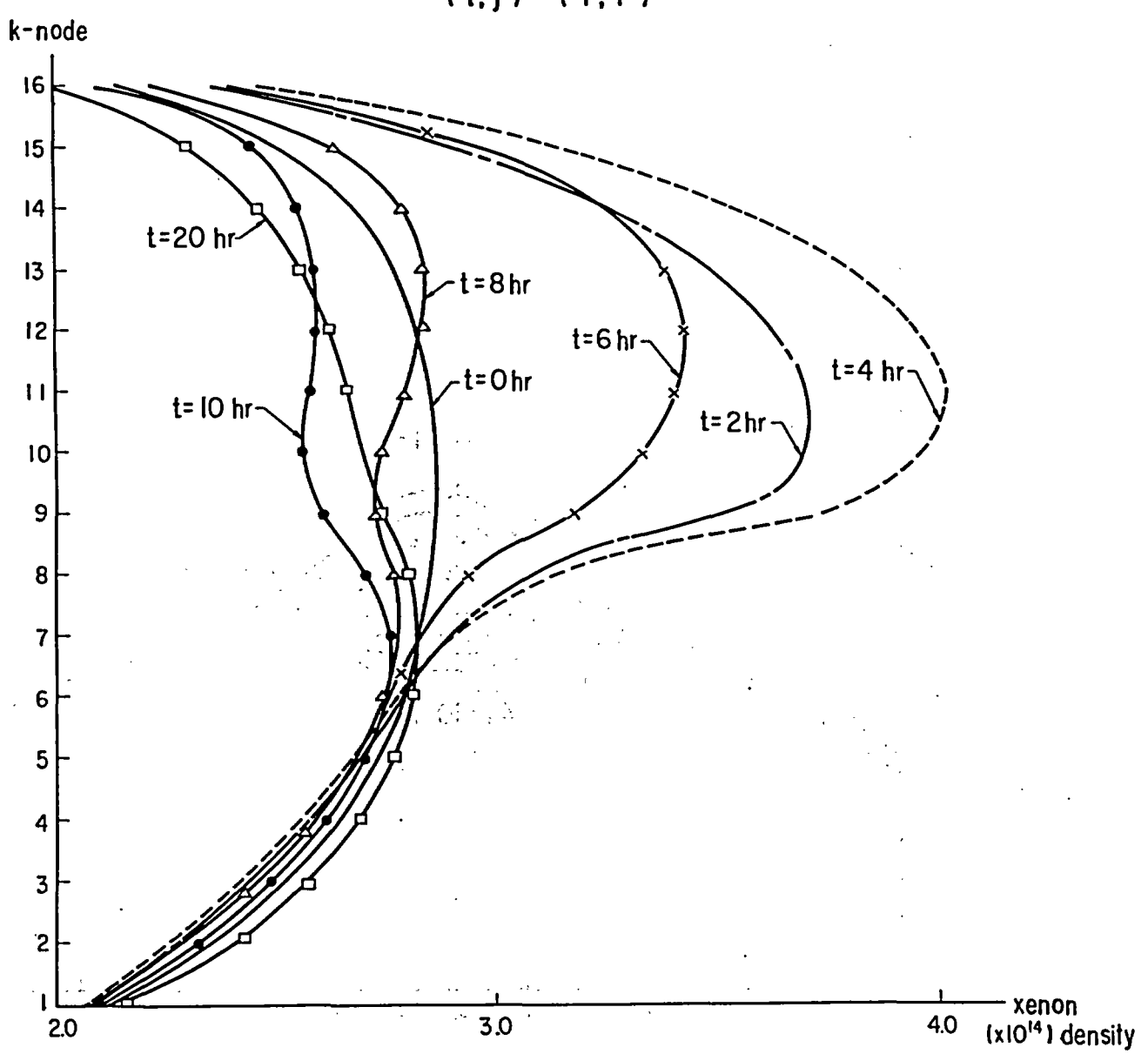

Fig. 10 Radial Xenon Distribution at Various Times during the Three-Dimensional Transient induced by the Half-Insertion (time = 0 hr) and Withdrawal (time = 6 hr) of the Flattening Rod in the (1 , 1) Channel

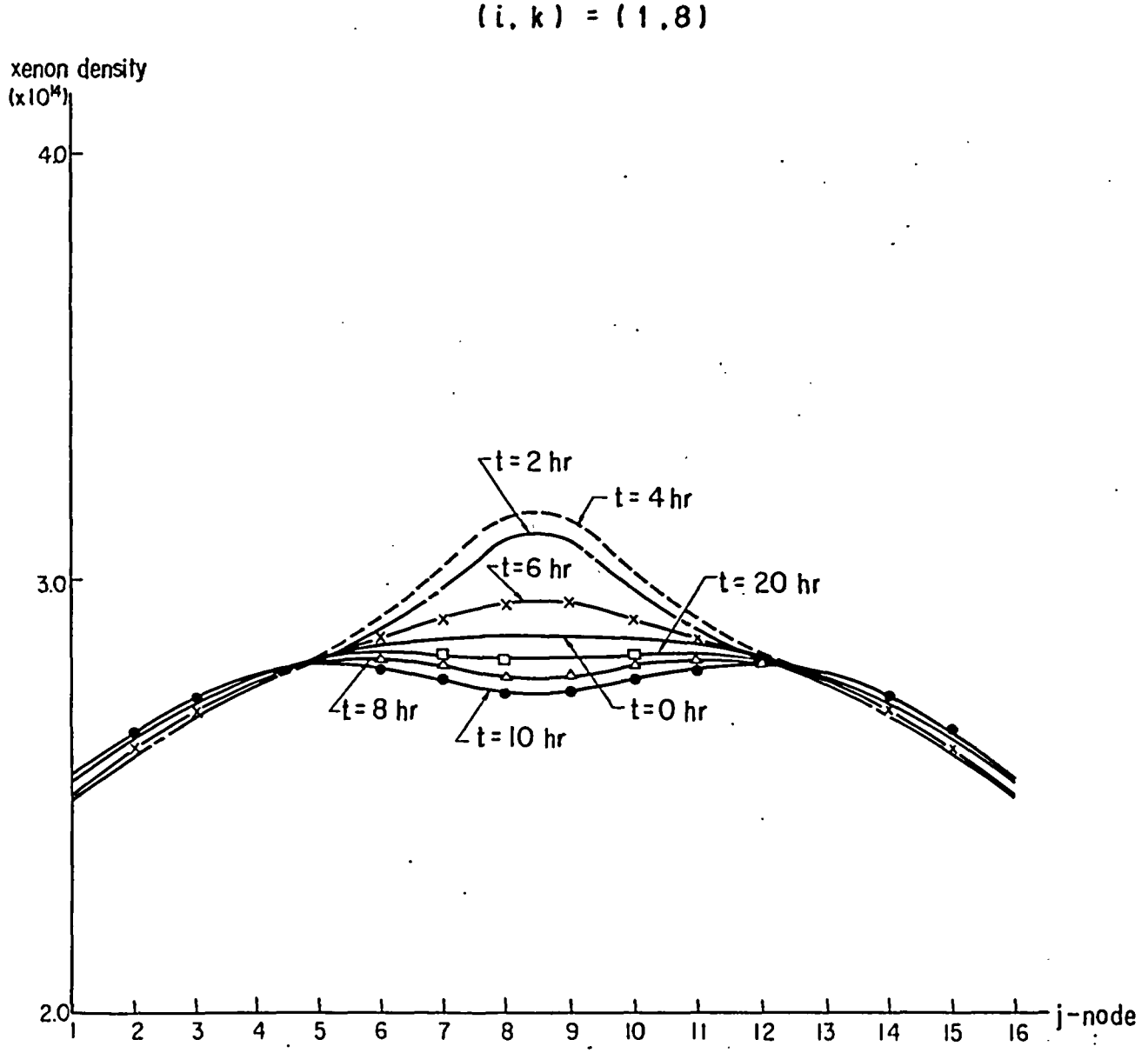

Fig. 11 Change of Eigenvalue at Various Times in Equilibrium Core induced by the Half-Insertion (time = 0 hr) and Withdrawal (time = 6 hr.) of Power-Flattening Rod and Power-Controlling Rods

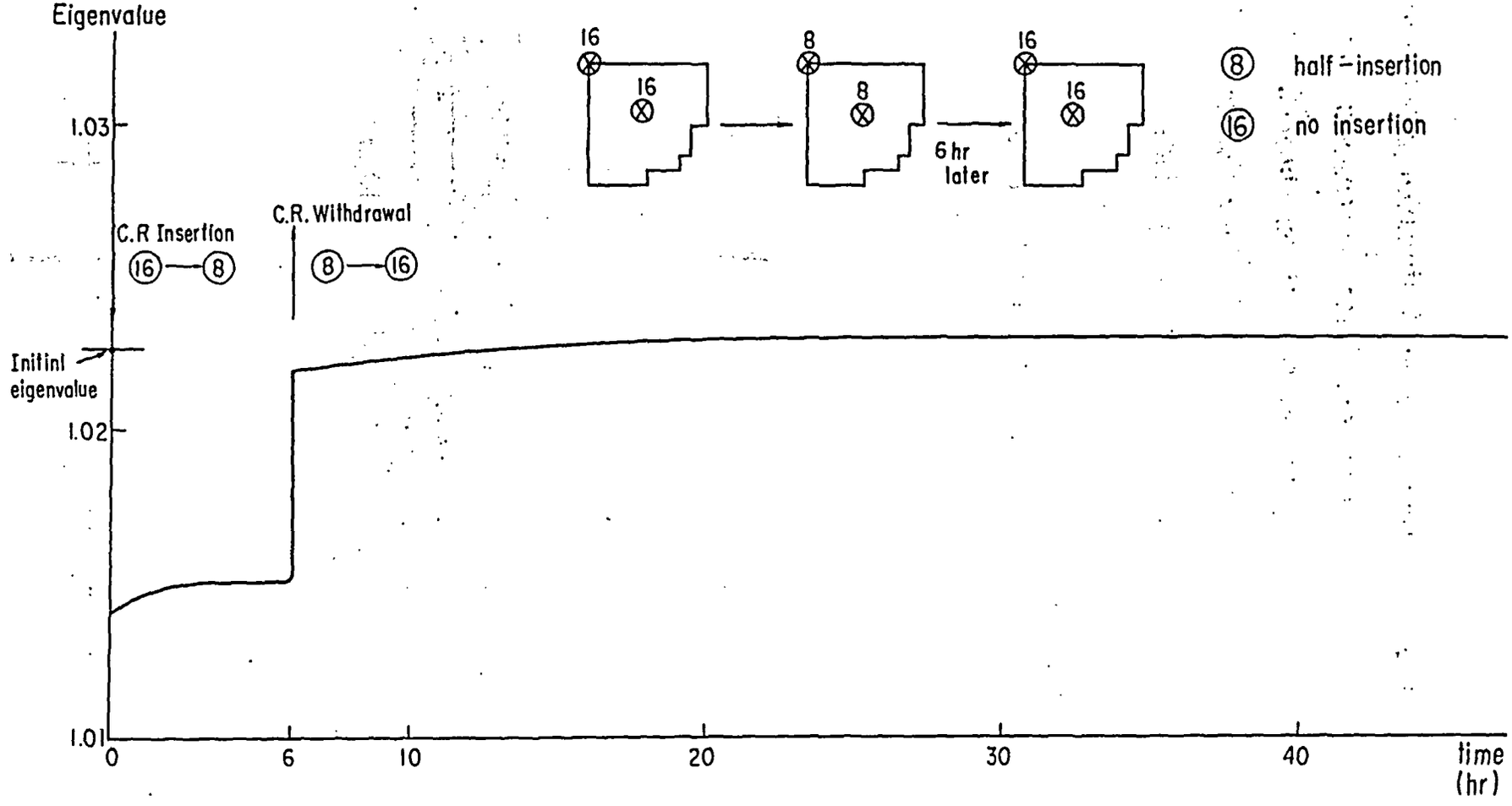

Fig. 12 Radial Xenon Distribution at Various Times during the Three-Dimensional Transient induced by the Half-Insertion (time = 0 hr) and Withdrawal (time = 6 hr) of Powe-Flattening Rod and Power Controlling Rods

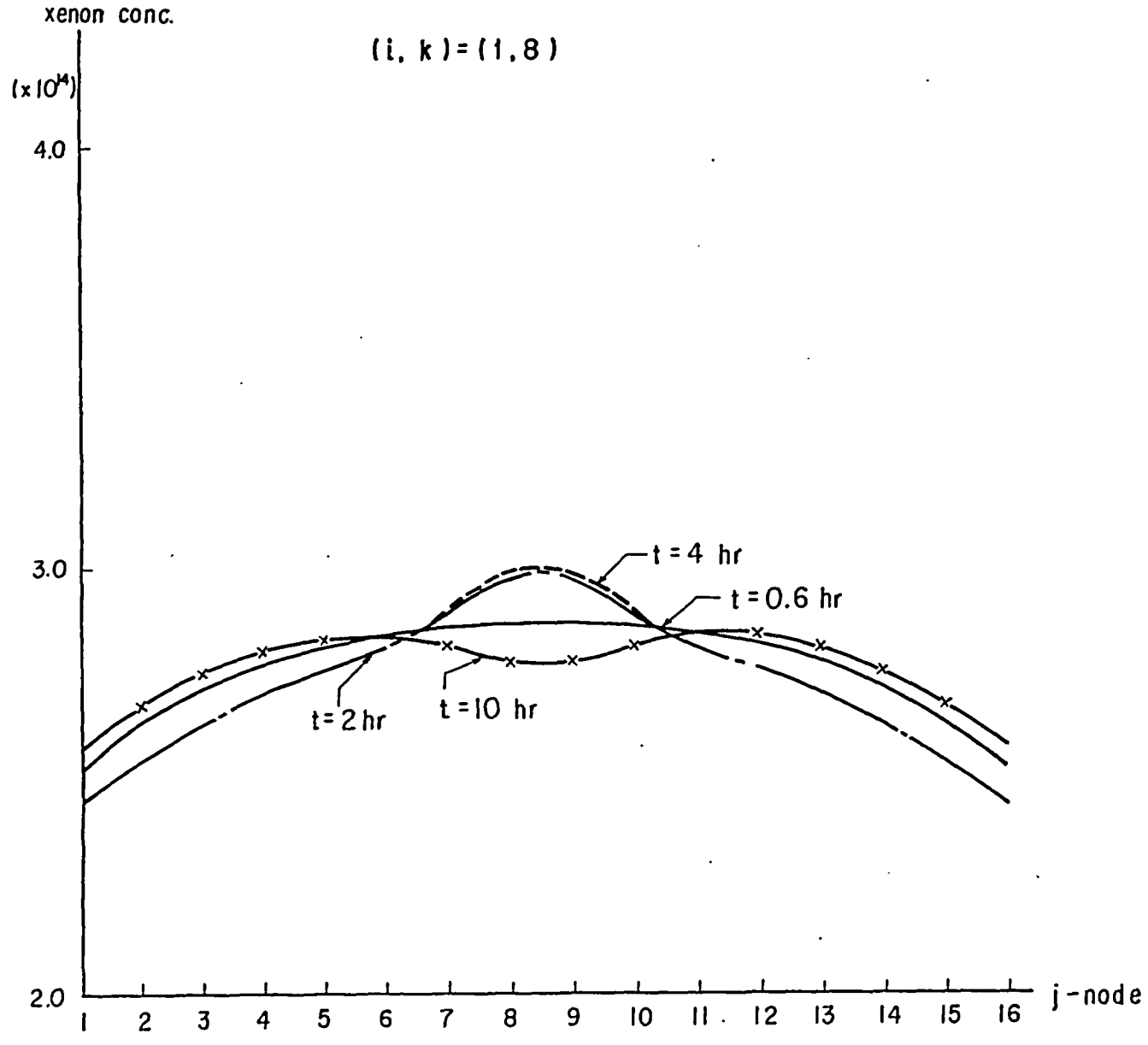

Fig. 13 Radial Xenon Distribution at Various Times during the Three-Dimensional Transient induced by the Half-Insertion (time = 0 hr) and Withdrawal (time = 6 hr) of Power-Flatting Rod and Power Controlling Rods

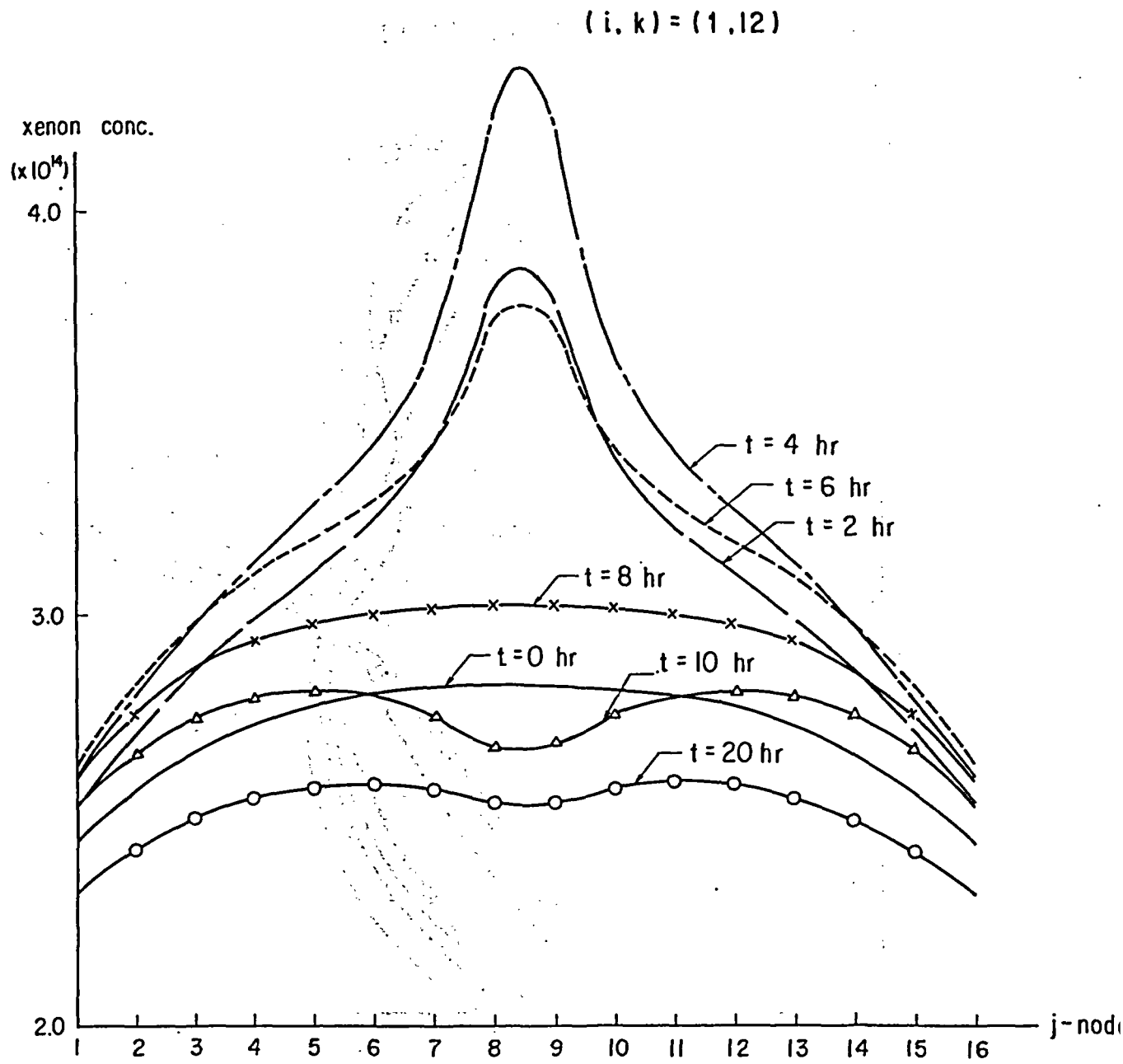

Fig. 14 Axial Xenon Distribution at Various Times during the Three-Dimensional Transient induced by the Half-Insertion (time=0 hr) and Withdrawal (time=6 hr) of Power Flattening Rod and Power-Controlling Rods

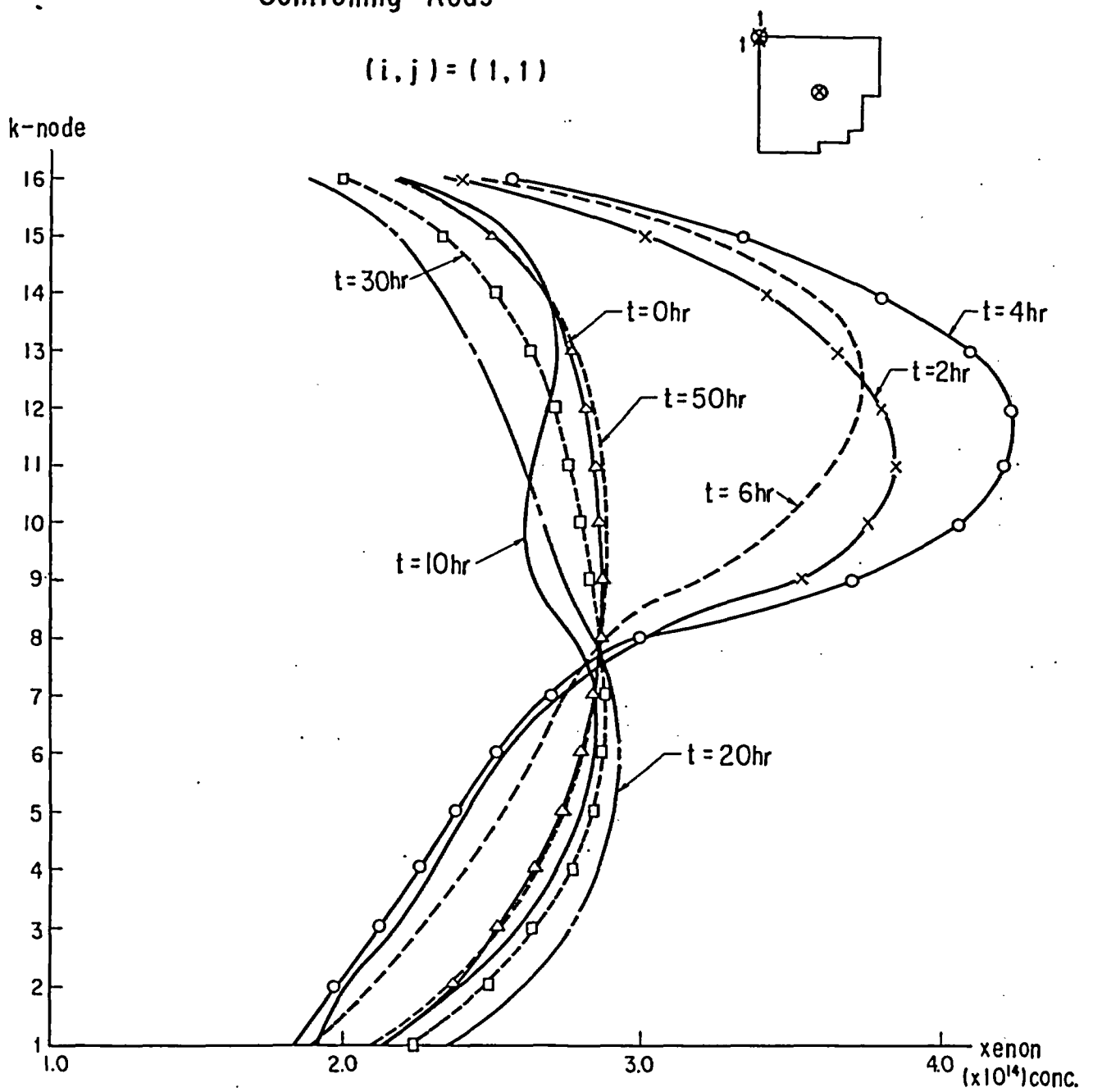

Fig. 15 Axial Xenon Distribution at Various Times during the Three-Dimensional Transient induced by the Half-Insertion (time = 0 hr) and Withdrawal (time = 6 hr) of Power-Flattening Rod and Power-Controlling Rods

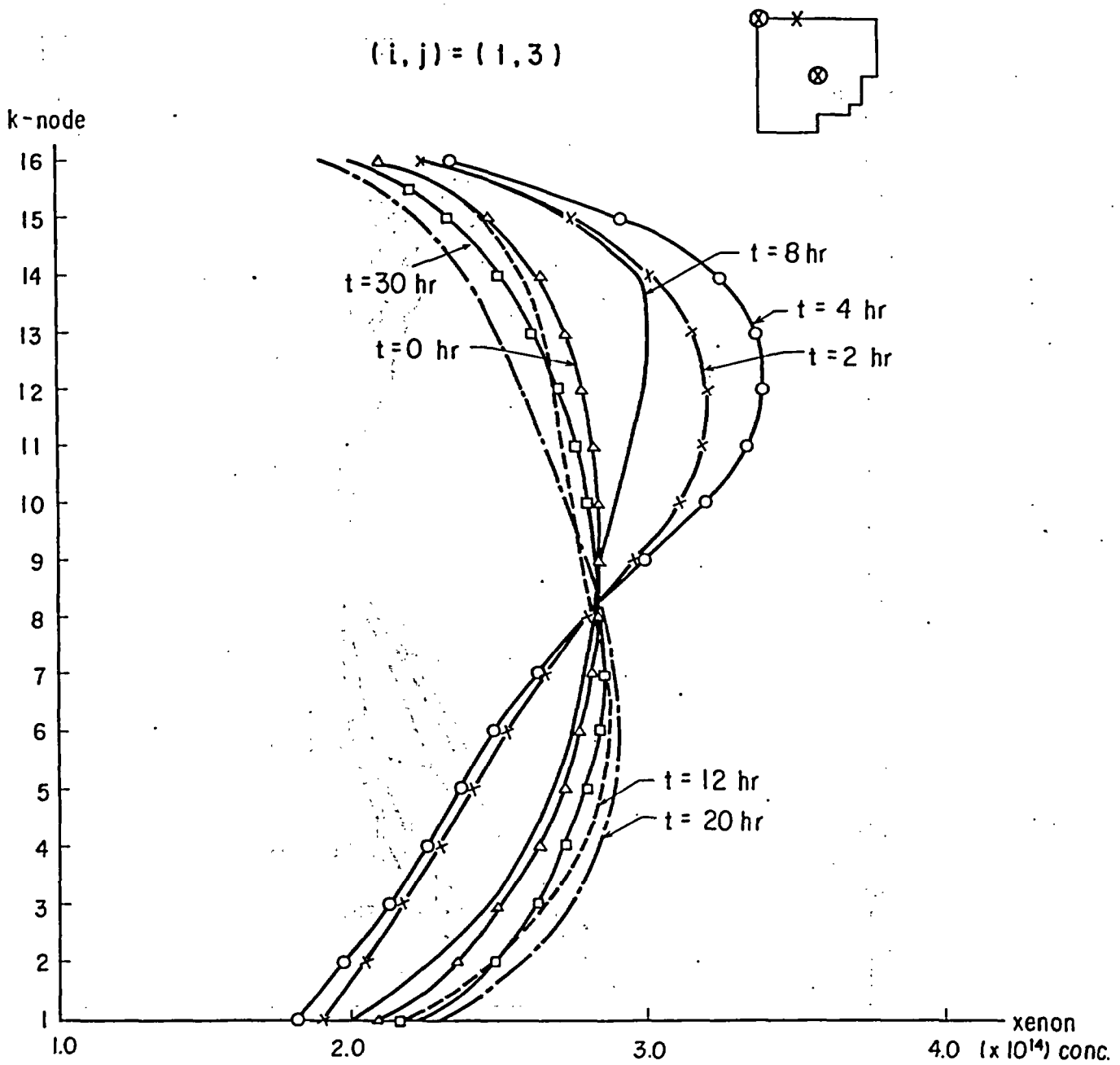

Fig.16 Axial Xenon Distribution at Various Times during the Three-Demensional Transient induced by the Half-Insertion (time = 0 hr.) and Withdrawal (time = 6 hr.) of Power-Flattening Rod and Power-Controlling Rods

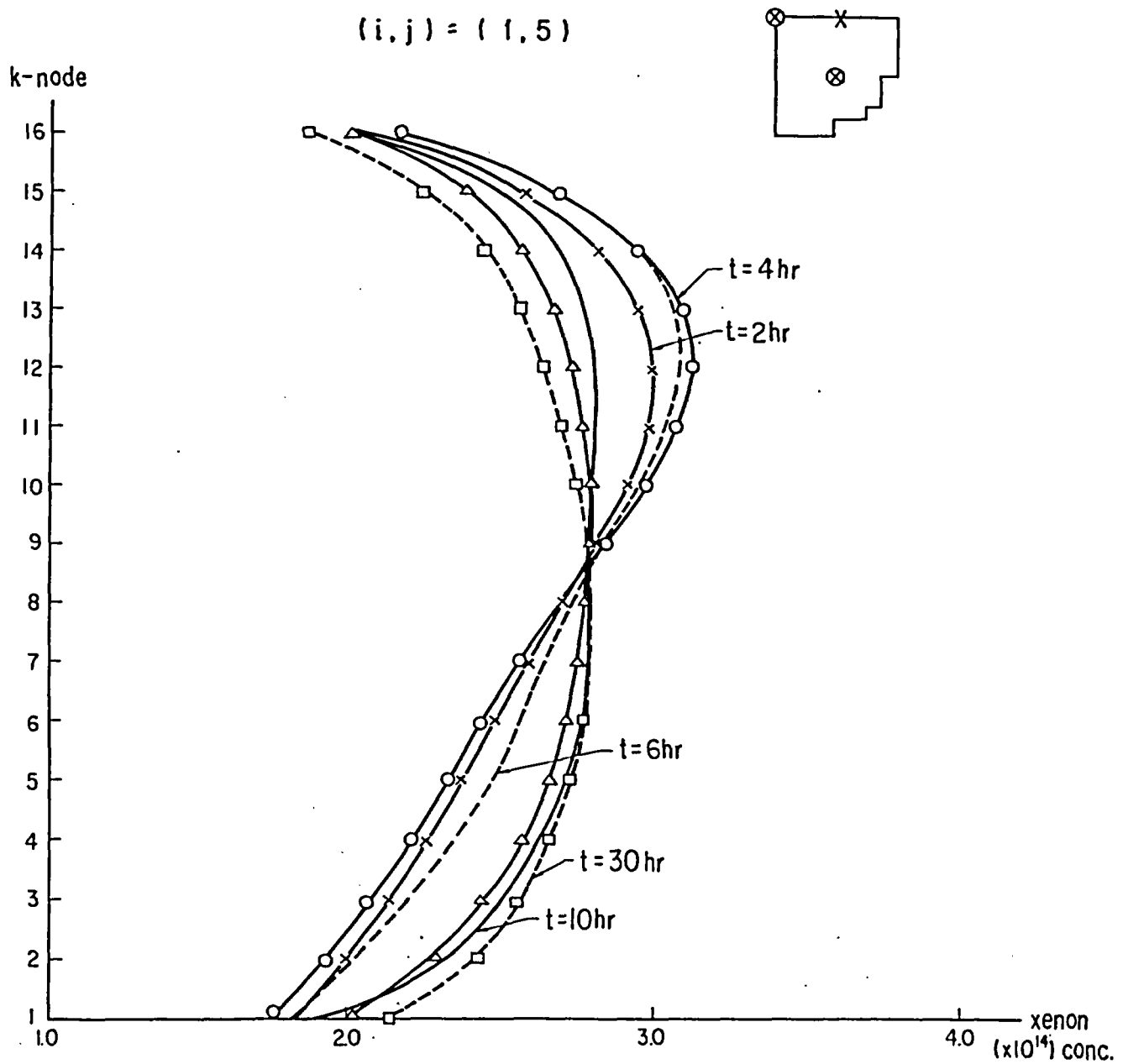

Fig.-17 Axial Xenon Distribution at Various Times during the Three-Dimensional Transient induced by the Half-Insertion (time = 0 hr) and Withdrawal (time = 6 hr) of Power-Flattening Rod and Power Controlling Rods

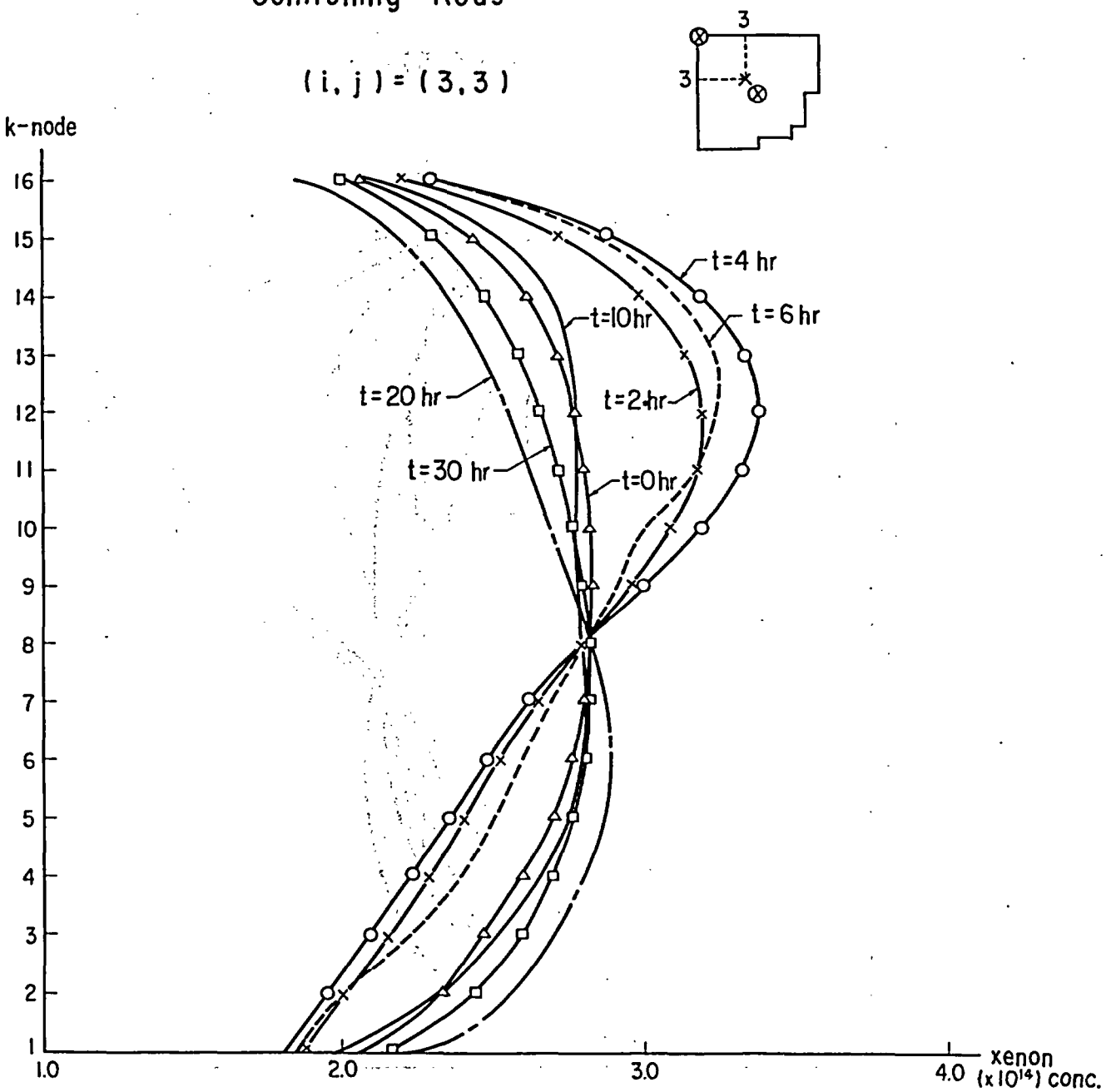

Fig. 18 Axial Xenon Distribution at Various Times during the Three-Dimensional Transient induced by the Half-Insertion (time = 0 hr) and Withdrawal (time = 6 hr) of Power-Flatting Rod and Power-Controlling Rods

(i, j) = (5, 5)

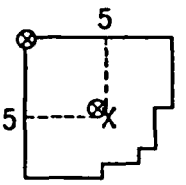

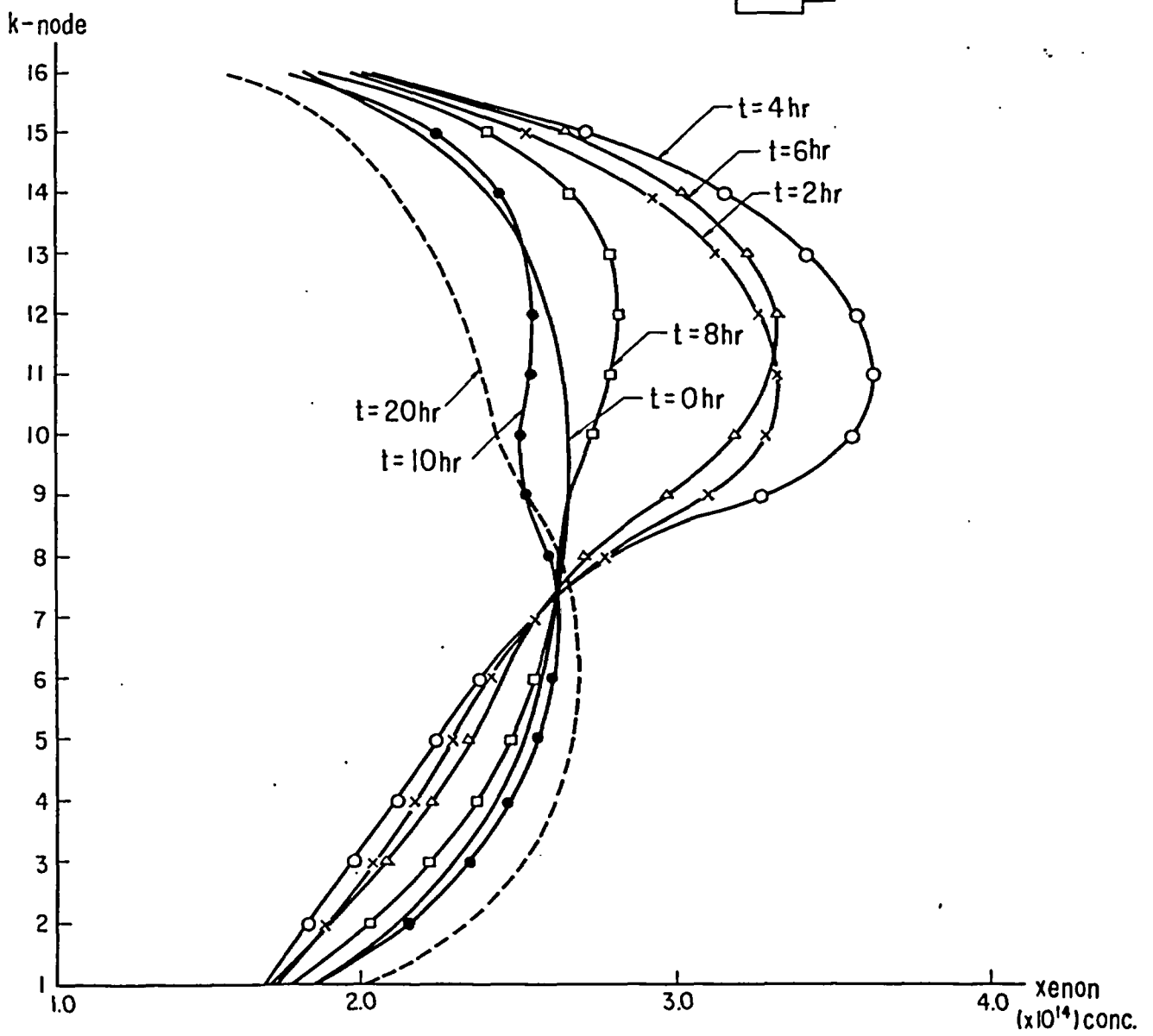

2. Xenon Override Studies

Contents

List of Figures

2.1 Introduction

The buildup of Xe^{135} following shutdown or power-reduction of high-flux thermal reactors with low excess reactivity may render these reactors subcritical for many hours. It has long been known that pre-shutdown power variations can modify the Xe^{135}, I^{135} transients to correct this problem.

In this paper, xenon poisoning induced by power-reduction is dealt with as well as xenon poisoning after shutdown. It is expected that on-power refueling is performed in the equilibrium core, so the problem of xenon poisoning induced by power-reduction has come to be very important from this point of view.

2.2 Three-Dimensional Analysis

The calculation of xenon poisoning can be carried out using the 'Improved' LAYMON Code; i.e., in this LAYMON Code, the principal improvements include general differential equations of xenon and iodine concentrations at any time. And in these equations, it is assumed that the flux drops to zero (or desired power-level) immediately when the reactor is shutdown (or is operated in the lower-level).

As a reactor can be shutdown from full to zero power in about a few minutes, this time is short compared with the several hours during which the xenon concentration builds up, and so very little error results from the assumption mentioned above.

In this paper, the calculation of xenon poisoning is solved in the 90° rotational symmetry core and is carried out in both the initial and equilibrium core defined in Chapter 2 of Part I.

The results of xenon poisoning calculations are listed in Table 1. Fig. 1 shows xenon buildup after the power-level change in initial core (557 MWt), Fig. 2 in initial core (635 MWt), and Fig. 3 in equilibrium core (635 MWt).

Table 1. Maximum xenon reactivity % $\left(\Delta K/K\right)$ and its time

Core / Power-level change	Equilibrium 635 MWt	Initial 635 MWt	Initial 557 MWt
100% → 80%	0.52% (5 hr)		
100% → 50%	1.76% (6 hr)	1.62% (6 hr)	1.40% (6 hr)
100% → 30%	2.76% (8 hr)	2.53% (8 hr)	
100% → 0%	3.52% (9 hr)	3.17% (9 hr)	2.61% (9 hr)

In the initial core, the whole control rod worth added to the reactor, due to the full-insertion of four Power-Flattening and the one-third-insertion of four Power-Controlling Rods, is about 2% $\left(\frac{\Delta K}{K}\right)$ (See Fig. 4).

In the equilibrium core, the whole worth, due to the full-insertion of one Power-Flattening and the half-insertion of four Power-Controlling Rods, is about 1% (Δk/k) (See Fig. 5).

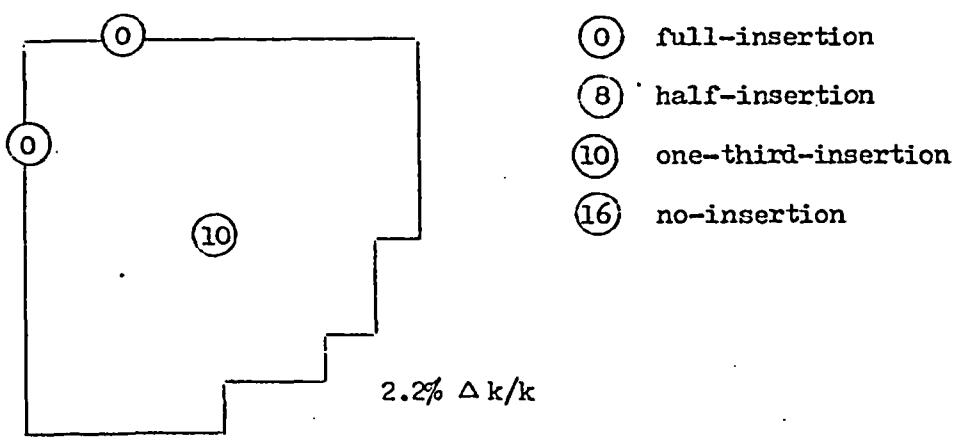

Fig. 4 Initial Core Control-Rods Pattern

Fig. 1 Xenon Buildup after the Shutdown or Power-Reduction in the Initial Core of 'FUGEN' (Thermal Power = 557 MWt, All Rods Out)

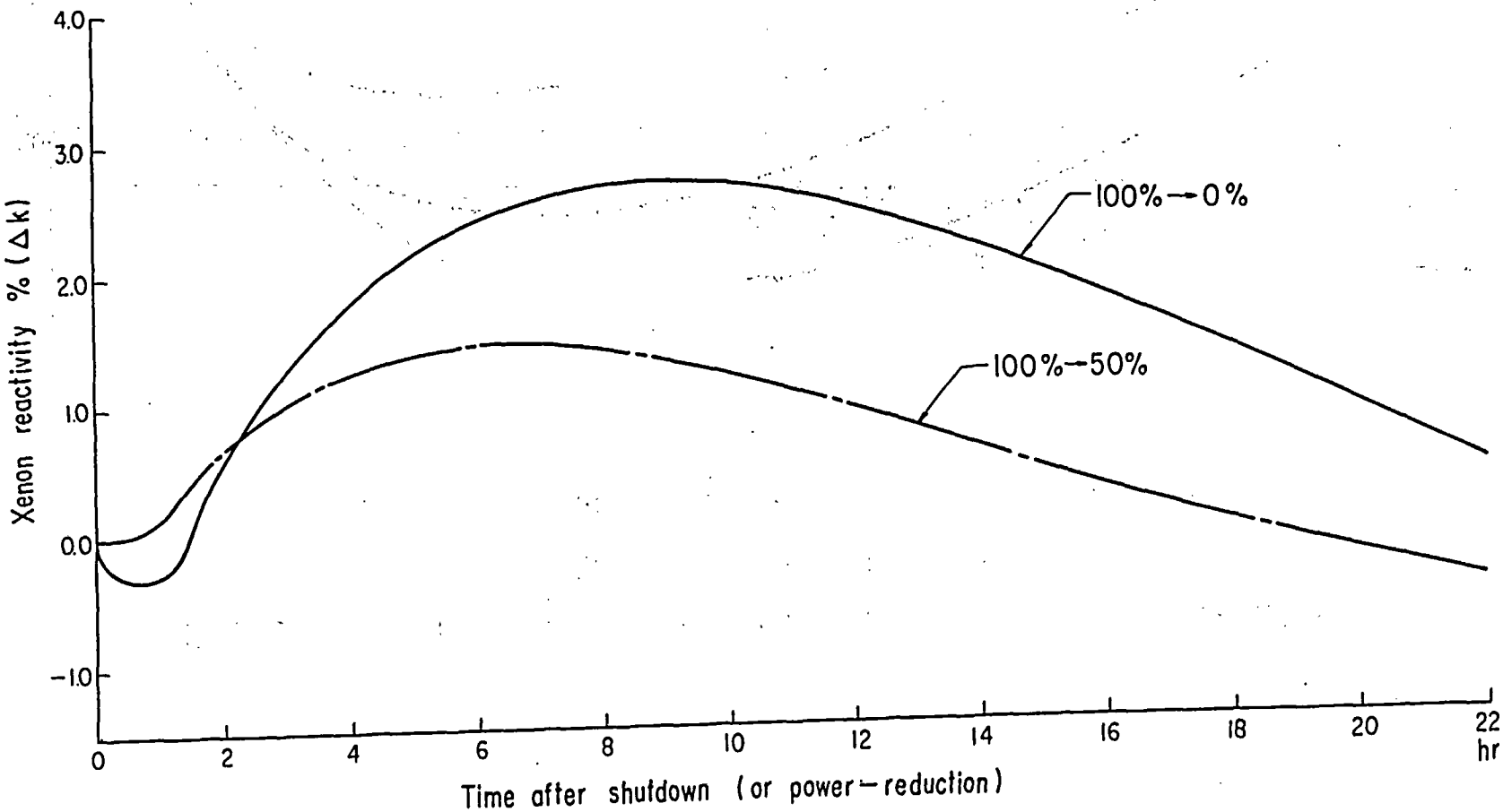

Fig. 2 Xenon Buildup after the Shutdown or Power - Reduction in the Initial Core of 'FUGEN' (Thermal Power = 635 MWt, All Rods Out)

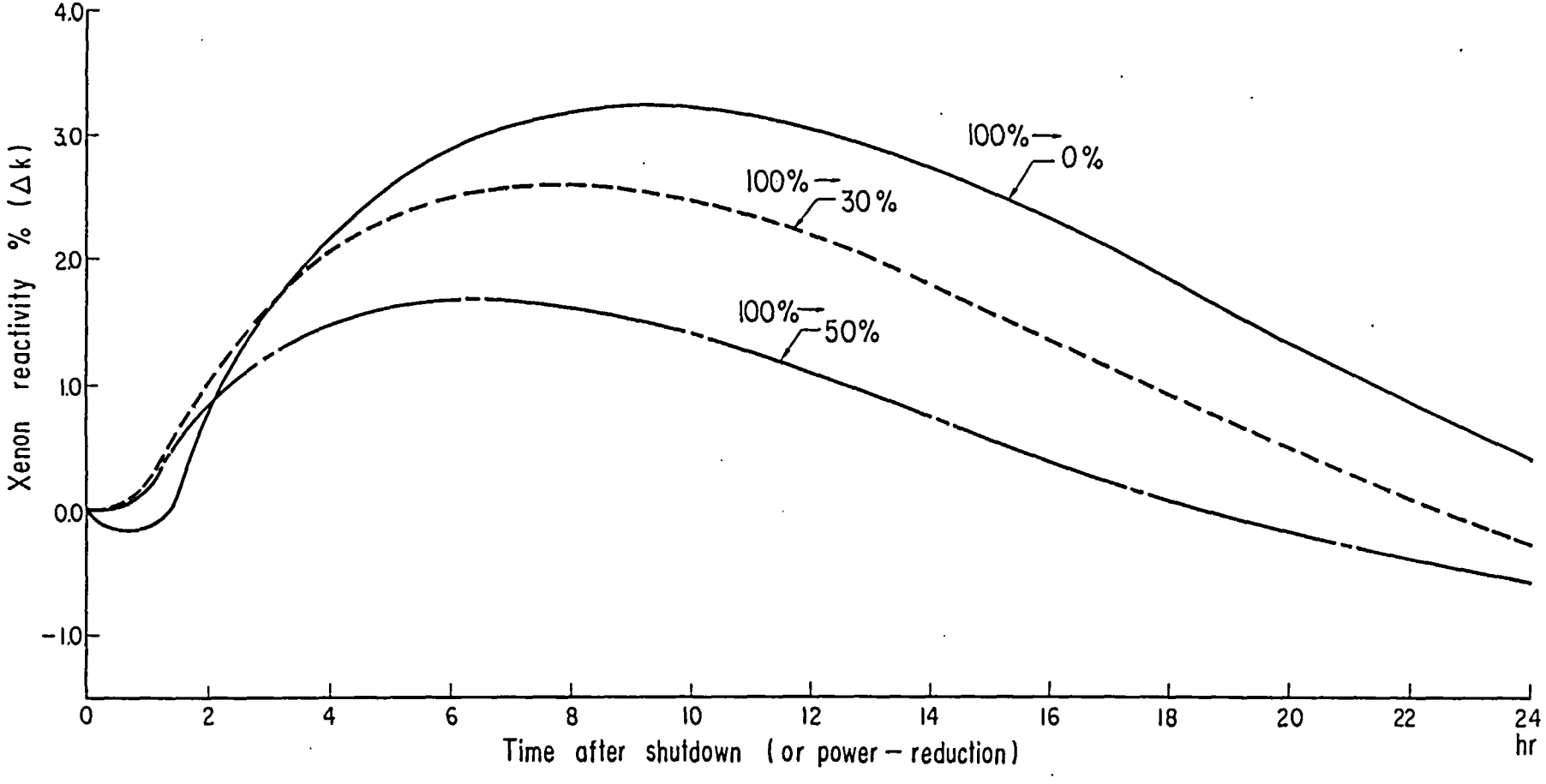

Fig. 3 Xenon Buildup after the Shutdown or Power-Reduction in the Equilibrium Core of 'FUGEN' (Thermal Power = 635 MWt, All Rods Out)

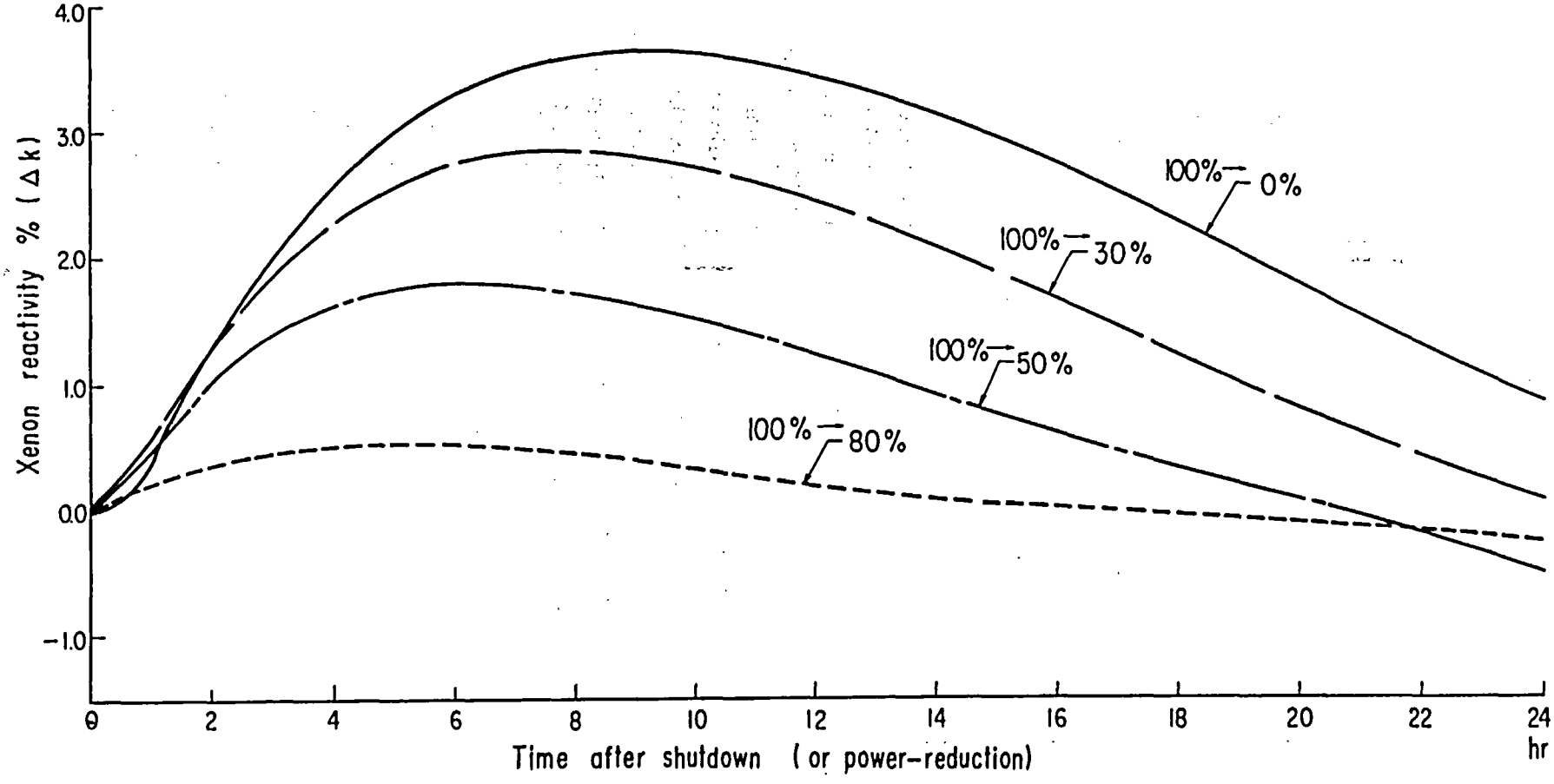

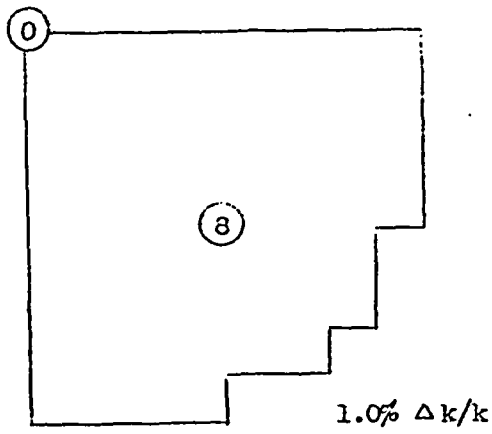

Fig. 5 Equilibrium Core Control-Rods Pattern

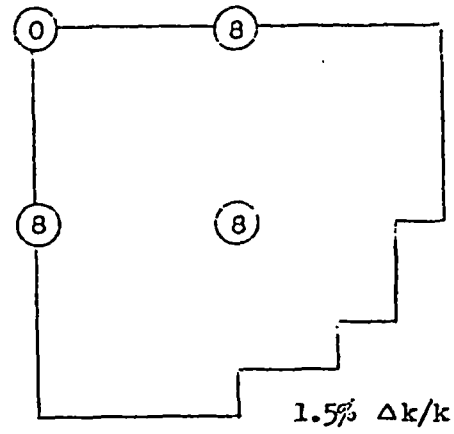

Fig. 6 Equilibrium Core Control-Rods Pattern with 1.5% Δk/k worth

According to the above description, it is possible to reduce the power-level in the initial core to 50 per cent of the full power and at most to 70 per cent in the equilibrium core. The operating margin of the control rods is designed to 2% $\Delta K/K$ as shown in Table 6 in section 3.4 of Part I, so if 1% $\left(\Delta K/K\right)$ control-rods worth is further added to the core, it is possible to reduce the power-level to about 50 per cent even in the equilibrium core. Fig. 6 shows equilibrium-core control-rods pattern with 1.5% / k/k control-rod worth for instance. And so it is necessary to determine the optimal control-rods pattern so that the demand is taken fully into account in the operation.